

NORTHWESTERN UNIVERSITY

Ethylene Glycol Reforming to Generate Hydrogen for Reduction of Nitric Oxide under
Lean Conditions over Supported Palladium Catalysts

A DISSERTATION

SUBMITTED TO THE GRADUATE SCHOOL
IN PARTIAL FULFILLMENT OF THE REQUIREMENTS

for the degree

DOCTOR OF PHILOSOPHY

Field of Chemical Engineering

By

Hiu Ying Law

EVANSTON, ILLINOIS

December 2007

ABSTRACT

Ethylene Glycol Reforming to Generate Hydrogen for Reduction of Nitric Oxide under
Lean Conditions over Supported Palladium Catalysts

Hiu Ying Law

The recent tightening of permissible NO_x release from diesel-powered engines has intensified the search for a catalytic system that can effectively remove NO_x under challenging diesel exhaust conditions. Hydrogen-assisted selective catalytic reduction (H_2 -SCR) using supported palladium catalysts offers significant promise for lean NO_x treatment due to its high activity at low temperatures. The origin of the superior activity of these supported Pd catalysts remains inconclusive. Practically, a source of H_2 needs to be secured onboard the vehicle since the H_2 concentration in the diesel exhaust is too low. In this thesis research, the feasibility of a coupled system consisting of an ethylene glycol (EG) reforming unit for H_2 production followed by H_2/CO -de NO_x unit was evaluated.

Na modified $\text{Pt}/\text{Al}_2\text{O}_3$ was studied for gas phase EG reforming at 230 °C to identify conditions to generate gaseous products suitable for NO_x reduction downstream. Addition of oxygen (O_2/EG above 0.9) to the reforming feed was found to prevent deactivation of $\text{Na}/\text{Pt}/\text{Al}_2\text{O}_3$ when EG concentration was 2.2%. H_2 contribution from WGS was insignificant

under our reforming conditions. Na modification of Pt/Al₂O₃ resulted in higher H₂ and CO₂ production, suggesting an enhancement in the WGS activity by Na.

Pd/Ti-PILC catalysts were selected for this study due to their high activity and selectivity. Pd/Ti-PILC catalysts with Pd loading between 0.1 – 0.5 wt% were prepared and tested for NO reduction activity with H₂-CO. The 0.1 wt% Pd/Ti-PILC was found to be most active and O₂-H₂ titration measurements indicate that this sample had a higher Pd dispersion compared to a Pd catalyst of a higher Pd loading. This suggests that the key parameter governing the activity of Pd supported catalysts for H₂-CO SCR of NO is the Pd particle size. The 0.1 Pd/Ti-PILC catalyst showed a large reduction in its ability to adsorb H₂.

SCR of NO using H₂ derived from EG reforming led to deactivation of Pd/Ti-PILC. The cause of deactivation was exposure to EG and can be circumvented by operating the reformer at an O₂/EG of 2.0 to achieve complete EG conversion.

ACKNOWLEDGMENTS

The last three years of research would not have been as interesting if it was not for the idea of this research proposal conceived by my advisors. The guidance and patience of Professor Harold H. Kung throughout this work is gratefully acknowledged. I would like to thank Professor Mayfair C. Kung for the catalysis knowledge and experimental skills she passed on to me. I have been fortunate to have two knowledgeable advisors.

Having the opportunity to work with Dr. Colleen Costello and Dr. Anguelina Kozlova when I first started was a wonderful experience. The technical assistance from Kris Popp, Dr. Shandong Yuan and Dr. Viorel Duma is much appreciated. I would like to thank my thesis committee members, Professors Peter Stair, Linda Broadbelt and Randall Snurr, as well as Professor Wolfgang Sachtler, for their insightful questions and helpful suggestions.

Numerous friends have been a source of support during this time. In particular, I would like to thank Deborah Robert, Carol Barker, Sharon Loy, Joanne Yao, Lily Soong and Jerry Hanttula. My family members have been extremely understanding and showed much concern for me, especially my uncle, Tak Ming Woo. I don't think he knows what an encouragement he has been to me during this time.

Most importantly, I would like to thank my mum, Sau Ling Woo. I would not have made it this far without her support, encouragement and love. All the encouragement and love that my father, John Law, gave me before he passed away have made it possible for me to reach this far.

TABLE OF CONTENTS

Abstract.....	2
Acknowledgments.....	4
Table of Contents.....	5
Lists of Figures.....	9
Lists of Tables.....	10
Chapter 1. Introduction.....	11
1.1 Evolution of NO _x Emission Control for Diesel Powered Engines.....	11
1.2 Current Technological Solutions for NO _x Removal.....	17
1.2.1 Lean NO _x Trap.....	17
1.2.2 Urea Selective Catalytic Reduction.....	18
1.2.3 Hydrocarbon Selective Catalytic Reduction (HC-SCR).....	19
1.3 Clay-based Catalysts for Lean NO _x Reduction.....	19
1.4 Hydrogen Assisted NO _x Reduction.....	20
1.5 Role of Hydrogen.....	21
1.6 Objective.....	21
1.7 Scope.....	22
Chapter 2. General Experimental Procedures.....	24
2.1 Catalyst Preparation.....	24
2.1.1 γ -Al ₂ O ₃	24
2.1.2 CeO ₂	24

	6
2.1.3 Pt/ γ -Al ₂ O ₃	25
2.1.4 Na/Pt/ γ -Al ₂ O ₃	25
2.1.5 Na/Pt/Ce/ γ -Al ₂ O ₃	26
2.1.6 Titania Pillared Clay (Ti-PILC).....	26
2.1.7 Pd/Ti-PILC.....	27
2.2 Reaction Studies.....	27
2.2.1 Reaction System.....	27
2.2.2 Data Analysis.....	29
2.3 Catalyst Characterization.....	30
2.3.1 Chemisorption Experiments.....	30
2.3.2 X-ray powder diffraction.....	31
2.3.3 Surface area measurements.....	32
 Chapter 3. Ethylene Glycol Reforming as a Source of Reductants for Catalytic NO _x removal.....	 33
3.1 Introduction.....	33
3.2 Experimental.....	36
3.2.1 Catalyst.....	36
3.2.2 Reaction Studies.....	36
3.3 Results and Discussion.....	37
3.3.1 Effect of O ₂ Concentration in EG Reforming.....	38
3.3.2 Effect of EG Concentration on H ₂ Production.....	43
3.3.3 Effect of Water Concentration on H ₂ Production.....	44

3.3.4 Effect of Na Modification of Pt/Al ₂ O ₃	51
3.5 Conclusion.....	56
Chapter 4. Parameter Controlling Activity and Pd Catalysts for H ₂ -Selective Catalytic Reduction of NO _x	57
4.1 Introduction.....	57
4.2 Experimental.....	59
4.2.1 Catalyst.....	59
4.2.2 Reaction Studies.....	60
4.3 Results and Discussion.....	61
4.3.1 Effect of Pd Loading on SCR of NO _x using a Simulated H ₂ -CO feed.....	61
4.3.2 Nitrogen Selectivity for H ₂ -CO SCR of NO.....	67
4.3.3 Effect of H ₂ O on NO _x Reduction Activity.....	68
4.4 Conclusions.....	70
Chapter 5. Low Temperature Lean NO _x Reduction by Coupling Ethylene Glycol Reforming with SCR.....	71
5.1 Introduction.....	71
5.2 Experimental.....	72
5.2.1 Catalyst.....	72
5.2.2 Reaction Studies.....	72
5.3 Results and Discussion.....	73
5.3.1 Coupled EG Reforming and deNO _x Reactions.....	73
5.4 Conclusions.....	80
Chapter 6. Conclusions and Recommendations for Future Work.....	81

	8
6.1 Conclusions.....	81
6.2 Recommended Work.....	84
6.2.1 H ₂ -CO SCR of NO.....	84
6.2.2 Ethylene Glycol Reforming.....	85
References.....	86

LIST OF FIGURES

Figure 1. Fuel Consumption and 3-way Performance of a Gasoline Engine as a Function of Air-Fuel (A/F) Ratio.....	14
Figure 3.1. Ethylene glycol reforming over 0.1 g Na/Pt/Al ₂ O ₃ at 230 °C as a function of time-on-stream. Feed: 410 ppm EG, 0.37% H ₂ O, balance N ₂ , total flow rate 107 mL/min.....	40
Figure 3.2. Ethylene glycol reforming over 0.1 g Na/Pt/Al ₂ O ₃ at 230 °C as a function of time-on-stream. Feed: 2.2% EG, 27.5% H ₂ O, balance N ₂ , total flow rate 46 mL/min.....	41
Figure 3.3. Ethylene glycol reforming over 0.1 g Na/Pt/CeO ₂ -Al ₂ O ₃ at 230 °C as a function of time-on-stream. Feed: 3.84% EG, 23.9% H ₂ O, 3.8% O ₂ , balance N ₂ , total flow rate 51 mL/min.....	50
Figure 3.4. Ethylene glycol reforming over 0.1 g Pt/Al ₂ O ₃ at 230 °C as a function of time-on-stream. Feed: 410 ppm EG, 0.37% H ₂ O, balance N ₂ , total flow rate 107 mL/min. Figure 3.3B: Deactivated catalyst after purging in nitrogen.....	53
Figure 4.1 NO _x reduction with Pd/Ti-PILC-B catalysts as a function of temperature. Reaction conditions: 500 ppm NO, 3000 ppm H ₂ , 1200 ppm CO, 5% O ₂ , total flow rate 210 ml/min. In each case, the amount of catalyst used corresponds to 0.0005g Pd.....	63
Figure 4.2 Effect of water on NO _x reduction at 185 °C. Reaction conditions: 3000 ppm H ₂ , 1400 ppm CO, 470 ppm NO, 5% O ₂ , 4% H ₂ O, total flow rate 200 ml/min, 0.5g 0.1wt% Pd/Ti-PILC-A.....	69
Figure 5.1 Coupled EG reforming-deNO _x reduction reaction. Reaction conditions for EG reforming: a feed of 2.2% EG, 2.65% O ₂ , 13.7% H ₂ O, total flow rate 77 mL/min, 0.1g Na-Pt/Al ₂ O ₃ catalyst, 230 °C. Reaction conditions for coupled-deNO _x : a feed of 1.4 % H ₂ , 3200 ppm CO, 1100 ppm EG, 500 ppm NO, 5.3% O ₂ , 5.3% H ₂ O, total flow rate 200 mL/min, 0.5g 0.1wt% Pd/Ti-PILC-B, 170 °C.....	75
Figure 5.2 Coupled EG reforming-deNO _x reduction reaction. Reaction conditions for EG reforming: a feed of 1.36% EG, 2.8% O ₂ , 8.5% H ₂ O, total flow rate 71 mL/min, 1.0g Na-Pt/Al ₂ O ₃ catalyst, 230 °C. Reaction conditions for coupled-deNO _x : a feed of 5400 ppm H ₂ , 960 ppm CO, 490 ppm NO, 5.8% O ₂ , 2.9% H ₂ O, total flow rate 200 mL/min, 0.5g 0.1wt% Pd/Ti-PILC-A, 185 °C.....	79

LIST OF TABLES

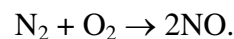
Table 1.1 Typical Compositions of Exhaust Gas from Lean-Burn Gasoline Engines and Diesel Engines.....	15
Table 1.2 Tier 2 Emission Standards, g/mi.....	16
Table 3.1 Oxidative reforming of EG at 230 °C over 0.1 g Na/Pt/Al ₂ O ₃	42
Table 3.2 Effect of EG concentration in EG reforming at 230 °C.....	44
Table 3.3 Effect of H ₂ O concentration in EG reforming at 230 °C.....	45
Table 3.4 WGS reaction over 0.1 g Na/Pt/Al ₂ O ₃ at 230 °C.....	46
Table 3.5 WGS reaction over 0.1 g Pt/CeO ₂ at 230 °C.....	48
Table 3.6 Oxidative Reforming of EG at 230 °C over 0.1 g catalyst.....	49
Table 3.7 Effect of Na Modification of Pt/Al ₂ O ₃ in EG Reforming.....	54
Table 4.1 Chemical Compositions of Bentonite and Ti-PILC determined by XRF.....	60
Table 4.2 Effect of Pd loading on NO _x reduction, CO and H ₂ conversions, N ₂ selectivity, NO _x reduction efficiencies.....	66
Table 4.3 Effect of H ₂ O on the NO _x Reduction Activity at 185 °C.....	68
Table 5.1 Effect of EG Concentration in the Reformer on NO _x Conversion at 170 °C in the Coupled Reactor Unit.....	76
Table 5.2 Effect of Exposure to Ethylene Glycol on the NO _x Activity of Pd/Ti-PILC at 170 °C.....	77
Table 5.3 Effect of EG Concentration on the EG Conversion and H ₂ Efficiency in EG Reforming.....	78
Table 5.4 Effect of O ₂ /EG ratio on EG Reforming over 0.3g Na-Pt/Al ₂ O ₃ , total flow rate 45 mL/min, 230 °C.....	78

CHAPTER 1: INTRODUCTION

1.1 Evolution of NO_x Emission Control for Diesel Powered Engines

In an attempt to prevent further damage to the environment, industrialized nations have put forth standards to regulate how much pollution may be emitted into the atmosphere. Nitrogen oxides (NO_x) is one of the principal air pollutants that is being regulated. Release of NO_x into the atmosphere contributes significantly to air pollution problems such as acid rain, depletion of ozone layer and smog, as well as respiratory diseases such as bronchitis and pneumonia [1].

NO is formed during combustion reactions at high temperatures between nitrogen and oxygen molecules to form various nitrogen oxides according to the overall reaction.



Nearly 30 million tons of NO_x are emitted annually [2]. As of 2003, manmade sources of NO_x such as electric utilities and other industrial, commercial and residential sources that burn fuels contribute towards 44% of this value [3]. But motor vehicles are responsible for the remaining 55%. Since the early 1970's, the U.S. Environmental Protection Agency (EPA) has stipulated motor vehicle manufacturers to reduce nitrogen oxides (NO_x) emissions from their products and these emission control policies have become progressively more stringent. As a result of the Tier 2 program, all cars, SUVs, pickups, and vans will be 77–95 percent cleaner by 2009.

One potential solution for NO_x removal is by NO decomposition which is thermodynamically favorable at temperatures below 1200 K. However, the activation energy for homogeneous NO decomposition is high (~ 335 kJ/mol) and a catalyst is needed for the reaction to proceed [4]. Up till 1986, catalysts used for NO decomposition suffered rapid poisoning due to competition of the NO adsorption sites by oxygen contained in the feed or that produced by NO decomposition. Even though progress in NO decomposition was made when Cu-ZSM5 was found to maintain its activity for this reaction [5], still the rate is not high enough for practical application. To date, no suitable catalyst with sustainable high activity has been found [6]. As a result, high reaction temperature and/or gaseous reductant is required to remove surface oxygen and regenerate catalytic activity. Other than NO decomposition, reduction of NO by reductants such as CO, NH_3 , hydrocarbons and H_2 offers an alternative for NO_x removal [2]. Current technology for NO_x cleanup has been based on this approach [7].

The major breakthrough in vehicle emission control technology came in 1980–81. In response to tighter standards, new gasoline powered cars were equipped with a “three-way” catalyst (TWC) that can simultaneously convert all three pollutants: CO and HCs to carbon dioxide and water while reducing NO to N_2 [8]. As of 2005, a typical TWC is composed of ~ 1 – 2% total precious metal (Pt and/or Pd and Rh), 20 – 25% high surface area CeO_2 , $\sim 12\%$ ZrO_2 to stabilize CeO_2 against sintering, and 50 – 55% is a Al_2O_3 washcoat deposited onto a ceramic monolith [9]. Addition of small amounts $\sim 6\%$ of metal oxides such as La_2O_3 [10] and $\sim 5\%$ BaO [11], if incorporated appropriately into the preparation process, improve the thermal stability of the Al_2O_3 . Pt and Pd are responsible for HC and CO oxidation, while Rh and Pd reduce NO to N_2 using CO and HCs in the exhaust. The less than 1 wt% NiO present acts as a scavenger for

H₂S, which is formed when sulfur oxides found in the exhaust are catalyzed by the TWC to H₂S [12].

The CeO₂ component has a number of functions: as an oxygen storage component (OSC), to improve precious-metal dispersion and reducibility and as a catalyst for water-gas shift reaction, steam reforming and NO reduction. For effective removal of NO, CO and HC to occur, the engine must operate under stoichiometric conditions, such that just enough oxygen is present to burn off all the HC, as shown in Figure 1 [13]. A shortage of O₂ leads to incomplete hydrocarbon combustion as well as the conversion of NO to NH₃, while an excess of O₂, i.e. lean conditions, result in incomplete NO conversion to N₂. But when the gasoline powered vehicles use an air-fuel mixture near the stoichiometric ratio of 14.7, TWCs can achieve more than 90% conversion of all three pollutants [14].

Besides controlling vehicle exhaust emissions, increasing fuel efficiency of combustion engines is the other major concern in automotive engine development. One way to enhance fuel efficiency is by operating the engines under lean conditions. Compared to gasoline powered engines operating under stoichiometric conditions, vehicles equipped with diesel or other lean burn engines offer 30% higher fuel economy [20]. Concurrently, the better fuel economy is accompanied by a reduction in the rate of CO₂ emission. Diesel and lean-burn engines release ca. 20 and 10% less CO₂ compared to conventional gasoline engines with closed loop TWC systems [15, 16]. This is another impetus of switching to lean burn engines since CO₂ emissions have been linked to global warming.

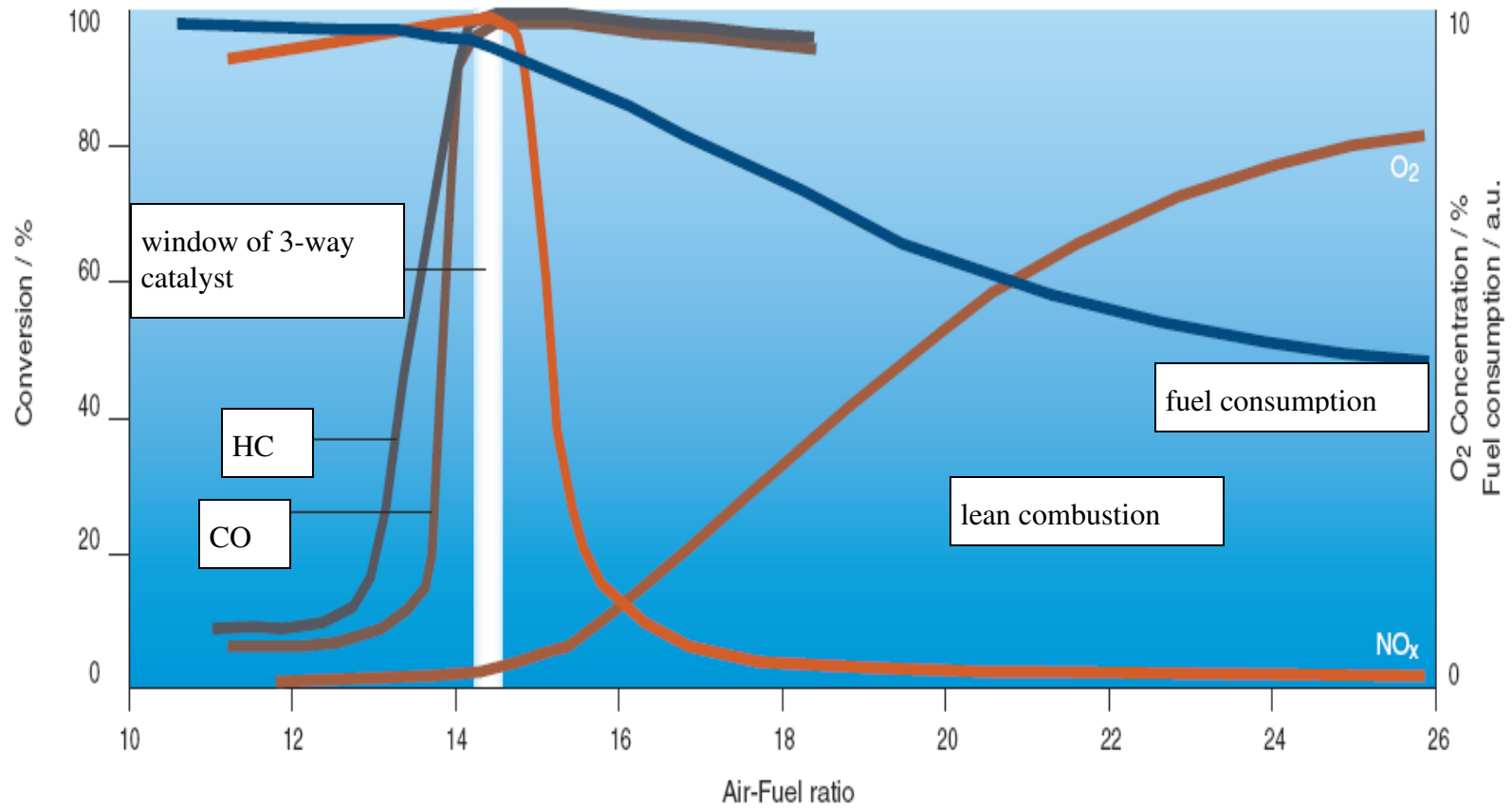


Figure 1 Fuel consumption and 3-way performance of a gasoline engine as a function of air-fuel (A/F) ratio.

However, lean engine operation makes NO_x removal from exhaust gas a very challenging task. The exhaust is too O_2 -rich for TWCs to be effective for NO_x removal under lean conditions. Table 1.1 presents the temperature range and typical exhaust compositions from diesel engines and from lean-burn gasoline engines [17-19]. From this table it is clear that an effective catalyst must not only be highly active and selective, but it must also maintain its activity in the presence of large concentrations of water and in the presence of SO_2 . Moreover, catalysts for diesel engines must be active at low temperatures, while catalysts for gasoline engines must be able to withstand high temperatures.

Table 1.1. Typical Compositions of Exhaust Gas from Lean-Burn Gasoline Engines and Diesel Engines.

Exhaust	Temp °C	NO_x %	O_2 %	HC ppm	CO ppm	H_2O %	Other
Lean-burn	400–700	0.002-0.15	4- 6	700	2000	9	SO_x CO_x
Diesel	200–400	0.002-0.07	4-10	7-27	200–300	5	SO_x CO_x particulate

Catalytic reduction of NO_x emissions from lean burn and diesel engines is difficult due to the large excess of oxygen in the exhaust gas and the low temperature of the gas. Widespread implementation of diesel engines is hindered by the inability to meet the stringent emission limits set by Federal regulations. Tier 2 standards, which were adopted in 1999, are detailed in Table 1.2. In particular, the current permissible NO_x limit is over 90% reduction compared to the previous Tier 1 standards.

Table 1.2. Tier 2 Emission Standards, g/mi [21, 22]

	NMHC ^a	CO	NO _x	PM ^b	HCHO
Tier 1	0.31	4.2	1.25	0.1	
Tier 2	0.09	4.2	0.07	0.01	0.018

NMHC^a – non-methane hydrocarbons

PM^b – particulate matter

When fully implemented in 2009, the average NO_x emissions of the entire light-duty vehicle fleet sold by each manufacturer must not exceed the NO_x standard of 0.07 g/mi. Several solutions have been proposed for controlling NO_x emissions from diesel-powered vehicles. One set of approaches focuses on the engine. Techniques such as exhaust gas recirculation are helpful, but these techniques alone will not eliminate NO_x emissions. Catalytic aftertreatment such as Selective catalytic reduction (SCR) is a potential solution for NO_x removal. SCR is a process in which a reducing agent reacts selectively with NO_x to produce N₂, in the presence of another oxidant, such as O₂. Such studies were first reported in 1990, when Iwamoto et al. [23] and Held et al. [24] independently studied HC-SCR of NO_x under lean conditions using Cu-ZSM-5.

Further testing, however, showed the Cu-ZSM-5 catalyst to be unstable under hydrothermal conditions. Since then, a large number of catalysts have been studied with the aim to discover better lean NO_x reduction catalytic systems. Perhaps the biggest challenge in lean NO_x reduction catalysis is for the hydrocarbon reductant to react selectively with NO instead of with the large excess of O₂ present in the exhaust. The competition between NO and O₂ for the reductant is closely related to the efficiency in SCR. Unlike the effluent from stoichiometrically operated gasoline engines, the concentration of unburned hydrocarbons and CO in diesel exhaust is much lower. Therefore, introduction of reductants into the exhaust is generally required for

effective NO_x reduction, thereby incurring a fuel economy penalty. Currently, peak NO_x conversion efficiencies for lean-burn catalysts are unacceptably low.

1.2 Current Technological Solutions for NO_x Removal

Thus far, the development a lean-burn NO_x catalyst that has the required activity and durability under the diesel exhaust operating conditions has proved to be a challenge. In spite of advances, there continues to be a need for an affordable and reliable exhaust treatment system, to be practically used to reduce NO_x emissions from diesel engines to a satisfactory extent to meet the present U.S. Environmental Protection Agency (EPA) regulations. The state of the art for automotive lean NO_x reduction can be grouped into the following: NO_x storage-catalyst (also referred to as lean NO_x traps, LNTs), urea selective catalytic reduction (urea-SCR) and hydrocarbon-SCR. However, these technologies have their shortcomings and efforts continue to improve them and to search for others [25].

1.2.1 Lean NO_x Traps

The NO_x storage catalyst is a key aftertreatment technology in use that combines NO_x adsorber catalysts with catalysts for NO_x reduction. This novel approach pioneered by Toyota, involves first converting the exhaust- NO_x to a solid nitrate stored on the catalyst under fuel lean conditions. To regenerate the catalyst, fuel rich exhausts are used for short intervals where the stored NO_x is removed through its reduction to N_2 , CO_2 and water. A typical LNT catalyst consists of Pt, Rh, barium, and a high surface area support, such as γ -alumina [26]. The Pt oxidizes NO to NO_2 to enhance the efficiency of the trapping reaction [27]. Rh is added to

facilitate the reduction of NO by CO [28]. Although LNTs have been implemented, issues such as deactivation of these systems due to sulfur poisoning and thermal aging remain to be solved [29, 30]. Furthermore, LNTs require advanced control systems for their periodic regeneration requirements.

1.2.2 Urea Selective Catalytic Reduction

The selective catalytic reduction (SCR) of NO_x with NH₃ under oxidizing conditions is a proven NO_x abatement technology for stationary applications. However, the NH₃-SCR technology is not suitable for mobile applications due to difficulty in handling and transportation of NH₃. Instead, aqueous urea is used to generate NH₃ in-situ as the active NO_x reducing agent. When the urea solution is injected into the NO_x-containing exhaust stream, the urea thermally decomposes into NH₃ and isocyanic acid (NHCO). The isocyanic acid formed from the thermal decomposition of urea readily undergoes catalytic hydrolysis to produce another molecule of ammonia [31]. The overall reaction for urea hydrolysis into ammonia is described by the equation below:



During the earlier 1980s, Kato et al. reported that NH₃-SCR is most effective when equimolars of NO and NO₂ are present [32].



One of the most promising catalysts for the SCR of NO_x by urea is the Cu-ZSM-5 catalyst [33]. Intense study in this area has led to the recent commercialization by DaimlerChrysler of the BlueTec technology, a urea-SCR based aftertreatment system for Euro IV HD trucks [34]. Although urea-SCR represents one of the best approaches for achieving aggressive NO_x reduction goals, implementation of this technology in the US would require setting up of infrastructure for urea distribution as well as devices in vehicles to prevent ammonia release in the tail gas.

1.2.3 Hydrocarbon Selective Catalytic Reduction (HC-SCR)

Selective catalytic reduction of NO using hydrocarbon has been studied extensively since the start of 1990. While reduction of NO_x using residual hydrocarbons present in the exhaust is the most ideal, these reactions do not show sufficient activities at the diesel exhaust conditions, especially the low temperatures. In addition, for HC-SCR, it is necessary to inject or to reform fuel for exhaust treatment since the concentration of the residual hydrocarbon is too low to reach the desirable level of NO_x removal.

1.3 Clay-based Catalysts for Lean NO_x Reduction

Pillared clay (PILC) based catalysts have been found to be excellent catalysts for the SCR reactions by ammonia (NH_3) and by hydrocarbons [35]. Using TiO_2 -PILC as a support, a 3/1 (molar ratio) of $\text{Fe}_2\text{O}_3/\text{Cr}_2\text{O}_3$ (total 10 wt%) showed an NH_3 -SCR activity twice as high as that of the commercial $\text{V}_2\text{O}_5/\text{TiO}_2$ catalyst [36]. For hydrocarbon SCR, Cu-ion-exchanged PILC yielded activities higher than that of Cu-ZSM-5. More significantly, its activity was only slightly

decreased by water and SO_2 [37, 38]. This is significantly different from Cu-ZSM-5 which is severely deactivated by water and SO_2 . Cu-exchanged pillared clay has also been found to be active for NH_3 -SCR [39].

1.4 Hydrogen Assisted NO_x Reduction

Prior the late 1990s, there have been very few reports on NO reduction by hydrogen mostly because for the catalysts studied, it was found that hydrogen reacts nonselectively with oxygen [40, 41]. Recently, there were a number of studies using hydrogen as a reductant over platinum-based catalysts [42, 43]. Yokota et al. [42] reported a NO_x conversion around 80% over a Pt/zeolite catalyst, with a nitrogen selectivity of 50%. The temperature of maximum NO_x conversion was at 120 °C. The same authors developed a Pt-Mo-Na/ SiO_2 catalyst which showed a considerable increase in nitrogen selectivity to 80% at the temperature of maximum NO_x conversion. Burch and Coleman investigated the $\text{H}_2/\text{NO}/\text{O}_2$ reaction over Pt/ Al_2O_3 and Pt/ SiO_2 catalysts. The SiO_2 supported catalysts was found to be active at lower temperatures and achieved a higher NO conversion of ~ 77% compared to the Al_2O_3 supported catalysts (~55%) [44]. The nitrogen selectivity for the Pt/ Al_2O_3 catalyst was ~55% at 140 °C. The nitrogen selectivity was not affected by the choice of support.

Ueda et al. studied Pt and Pd catalysts on various supports for the $\text{H}_2/\text{NO}/\text{O}_2$ reaction in the presence of 10% water [45, 46]. The Pt/ Al_2O_3 catalyst reached a maximum NO conversion of 62% at 100 °C. All the supported Pd catalysts showed two distinct NO conversion maxima, one centered at 100 °C and the other at 300 °C. The low temperature peak was assigned to reaction

between H_2 and NO, while the high temperature peak was assigned to reaction between H_2 and in situ generated NO_2 . The maximum NO conversion was found to vary significantly with the choice of support: the Pd/TiO₂ catalyst outperformed the Pd/Al₂O₃ catalyst. Although supported Pt catalysts show high activity for H_2 reduction of NO, the NO reduction activity suffers tremendously when CO is present [47].

1.5 Role of Hydrogen

NO dissociation, which could possibly be the rate-determining step, was enhanced in the presence of hydrogen [48-50]. It has been proposed that hydrogen could possibly enhance the rate of migration of isocyanate species from the metal to the support via gas-phase HNCO [51]. A detailed study of the reaction mechanism for H_2 -SCR of NO over supported Pd catalysts was carried out by Macleod et al. [51]. Briefly, both the low and high-temperature mechanisms generate NH_3 in situ. The low-temperature channel operates via formation and subsequent hydrolysis of NCO species while the high temperature channel forms NH_3 directly from reaction between H_2 and NO.

1.6 Objective

The literature reviewed in this chapter show that even the most aggressively pursued NO_x technologies have their drawbacks that impede their implementation. Recently, hydrogen-assisted NO_x removal was suggested as a promising method to meet diesel emission standards with the potential to overcome the drawbacks associated with the current technologies for diesel exhaust NO_x removal. Although hydrogen is an effective reductant at low temperatures, its concentration in the exhaust is too low.

The goal of this research is to determine the feasibility of gas phase reforming of ethylene glycol (EG) under conditions amenable to vehicle applications. One significant advantage of EG compared to fossil fuel as a H₂ source is that EG can be readily manufactured from sources such as sugars or sorbitol, thus making EG a renewable reductant. Specifically, the aim is to identify conditions for which a stable and high hydrogen production is achieved.

Supported Pd catalysts possess high activity and selectivity for H₂-SCR of NO. However, the origin of the activity is not well understood. Moreover, the existing model of the active site in the literature cannot be used to explain the vast difference in the NO reduction activity over catalysts with similar compositions. In this respect, we aim to develop a model of the active center, one that could potentially explain the difference in the reported activities. This was achieved by preparing catalysts with different Pd loading, so as to obtain catalysts with different Pd dispersions. Chemisorption studies were conducted to obtain Pd dispersion information.

After optimization of the reforming and the deNO_x subunits separately, they were integrated to form a coupled system. The effect on NO reduction using reductants (H₂/CO) derived from EG was demonstrated.

1.7 Scope

The general experimental procedures, which include details of catalyst preparation, a description of the reaction test system, analysis of the reaction data, procedures for characterization of the catalysts, are described in Chapter 2. Chapter 3 describes the study of gas phase ethylene glycol reforming to produce hydrogen for NO reduction downstream. The effect of ethylene glycol, oxygen and water concentration on the hydrogen production as well as the

modification of the reforming catalyst with Na was studied. The effect of Pd loading on the NO reduction activity of supported Pd catalysts by H₂ and CO is presented in Chapter 4. The Pd dispersion of these catalysts was obtained by titration measurements. Chapter 5 presents the coupling of ethylene glycol reforming to a H₂/CO-SCR unit and modification of the reforming conditions to prevent deactivation of the deNO_x catalyst.

CHAPTER 2: GENERAL EXPERIMENTAL PROCEDURES

2.1 Catalyst Preparation

2.1.1 γ -Al₂O₃

The large pore γ -Al₂O₃ support used in this study was prepared similar to the procedure of Maeda et al. [1]. 100 g of aluminum isopropoxide (Aldrich, 99.99+%, white powder) was mixed with 214 g of the chelating agent tetraethylene glycol dimethyl ether at 100 °C. The temperature was raised to 120 °C for 7 hr to effect the ligand exchange reaction. Afterwards, the mixture was cooled to 90 °C and hydrolyzed with 10 fold excess water. After aging at 90 °C for 6 hr, the solid was filtered, washed with 2-propanol and air dried. It was then calcined in a large U-tube quartz reactor in flowing air to 700 °C at a heating rate of 1 °C/min and held at 700 °C for 2 hr. At 500 °C, 2% water was introduced into the air stream. The alumina was cooled to room temperature in dry flowing air. From the N₂ adsorption isotherm, it was determined that 80% of the pore volume was associated with a pore size diameter 10 Å and greater. The BET surface area of the resulting γ -Al₂O₃ was 235 m²/g. The pore volume measured by wetting with water was 3.8 mL/g. This γ -Al₂O₃ support was prepared by Professor Mayfair Kung.

2.1.2 CeO₂

Ceria support of better homogeneity and higher surface area (surface area of 125 m²/g) was prepared by the urea-co-precipitation-gelation method similar to that of Amenomiya et al [2]. More homogeneous precipitation is achieved by slow urea decomposition. Appropriate amounts of Ce(NO₃)₃·6H₂O (Alfa Aesar, 99.5%) and urea (Alfa Aesar, 99.5%) were dissolved in 900 mL of deionized water. 30 mL NH₄OH (Alfa Aesar, 28-30% NH₃) was added dropwise (~1 mL/min).

The mixture was heated at 100 °C with constant stirring. The precipitate was filtered, then washed with 600 mL of boiling deionized water and dried in an oven at 110 °C overnight. The sample was ground and calcined at 400 °C for 4 hr. The high surface area ceria support used for the WGS reaction was prepared using a procedure similar to that of Li et al [3].

2.1.3 Pt/ γ -Al₂O₃

1 wt% Pt/ γ -Al₂O₃ catalysts used for EG reforming were prepared by incipient wetness method using an aqueous solution of tetraamine platinum(II) nitrate (Pt(NH₃)₄(NO₃)₂, Alfa Aesar). The Pt precursor was dissolved in de-ionized distilled H₂O and added dropwise to γ -Al₂O₃ flowing in a rotating beaker. Once impregnation is complete, the resulting catalyst was dried under a flood lamp until the solid flowed freely again. The solid was dried at 110 °C overnight and then calcined at 260 °C for 2 hr.

2.1.4 Na/Pt/ γ -Al₂O₃

The Na/Pt/ γ -Al₂O₃ catalyst was prepared by adding an aqueous solution of Na₂CO₃ to Pt/ γ -Al₂O₃ by incipient wetness to achieve 1.4 wt% Na loading. The final solid was dried at 110 °C overnight, then calcined to 400 °C. The effect of Na addition to Pt/ γ -Al₂O₃ is discussed in Chapter 3.

2.1.5 Na/Pt/Ce/ γ -Al₂O₃

8.3 wt% ceria was added onto a high surface area aluminum oxide (267 m²/g). From calculations assuming a linear structure of CeO₂, addition of this amount of ceria is close to one monolayer of ceria on Al₂O₃.

2.1.6 Titania Pillared Clay (Ti-PILC)

The titania pillared clay support was prepared in a similar manner as that described by Sterte [4]. Two batches of Ti-PILC prepared with different amounts of Ti were prepared. To prepare the pillaring solution, TiCl₄ (Aldrich) was first added to a 2 M HCl solution, and then de-ionized distilled (DDI) water was added slowly while the solution was vigorously stirred until the final Ti concentration reached 0.82 M for one sample (Ti-PILC-A) and 0.66 M for the other (Ti-PILC-B), and the final HCl concentration was 0.11 M. The partially hydrolyzed Ti-polycation solution was aged for 12 hr at room temperature before use. Meanwhile, 4 g of a purified montmorillonite powder (Bentonite, Fisher) was dispersed in 1 liter of DDI water for 5 hr with vigorous stirring. Then, the Ti pillaring solution (10 mmol Ti/g clay) was added slowly with vigorous stirring to the clay suspension. Intercalation was allowed to take place for 18 hr after which the mixture was suction filtered. The solid was washed with DDI H₂O and resuspended in DDI H₂O repeatedly until the filtrate was free of chloride ions. The sample was dried at 120 °C overnight and calcined at 300 °C for 12 hr. The clay was ground and sieved before being impregnated with Pd.

2.1.7 Pd/Ti-PILC

Pd was added to the Ti-PILC by incipient wetness using aqueous solutions of palladium (II) nitrate (Aldrich). A batch of catalysts of 0.1, 0.2 and 0.5 wt% Pd loading was prepared with Ti-PILC-B, and another batch of 0.1 wt% Pd was prepared with Ti-PILC-A. After impregnation, the solids were dried at 120 °C overnight and then calcined at 500 °C for 6 hr.

2.2 Reaction Studies

2.2.1 Reaction System

EG reforming and deNO_x were carried out in two independently controlled but connected reforming and deNO_x reaction units, such that the products from the reforming unit could be fed to the feed stream of the deNO_x unit. The reactions were carried out in a flow system at near atmospheric pressure. The flow rate of each gas was controlled by mass flow controllers (Brooks, model 5850C). The powder catalyst samples were held in place between two quartz wool plugs in U-shaped quartz reactors that were placed in homemade quartz furnace controlled by a Eurotherm temperature controller (model 2416). The tips of the thermocouples were attached outside the reactors but in contact with the middle section of the catalyst beds to monitor the catalyst temperature during reaction, which were also used to control the electric furnaces. All thermocouples used were K-type (chromel-alumel alloy). A pressure gauge located upstream of the reactor was used to monitor the system pressure. All reactor lines were heated to 100 °C to prevent condensation.

All EG reforming reactions were typically conducted at 230 °C. Ethylene glycol (Alfa Aesar) and de-ionized distilled H₂O were injected directly into the quartz wool upstream of the catalyst bed in the reforming unit using a Harvard syringe pump. N₂ (ultra high purity, Airgas) and O₂ (20% O₂ /N₂, Matheson) were used as purchased. The feed composition was adjusted using the liquid injection rate and the gas flow rates, while maintaining the total flow rates to within the range of 30 – 77 mL/min, unless otherwise stated. Typically, the catalysts were heated in a stream of nitrogen to the desired reaction temperature.

For experiments with low EG concentrations in the reforming feed, EG was introduced by bubbling a stream of N₂ through a heated saturator containing EG. The EG in the saturator was maintained at 65 °C by an insulated water jacket. Likewise, water vapor was added to the reforming feed by separately bubbling a stream of N₂ through a water saturator containing de-ionized distilled water at 50 °C. The N₂ flow rates were adjusted to yield a feed composition of 410 ppm EG, 0.37% H₂O, balance N₂ with a total flow rate of 107 mL/min.

For SCR of NO_x using a simulated H₂/CO feed, H₂ (2% H₂/Argon, Airgas), CO (5% CO/Argon, Matheson), and NO (1% NO/Helium, Matheson) were used as purchased. The flow rates of these gases were adjusted to form a 200 mL/min feed stream containing 500 ppm NO, 3000 ppm H₂, 1200 ppm CO, 5% O₂ and when present, 4% H₂O. For NO_x reduction using EG reformat in the coupled system, the reformat stream leaving the reforming reactor was combined with a simulated exhaust stream containing NO, O₂ and N₂, such that the 200 mL/min stream entering the NO_x reactor was composed of 3640–14000 ppm H₂, 0–3200 ppm CO, 2.9–6.8% H₂O, 500 ppm NO, and 5–5.8% O₂.

The compositions of the feed and product streams were analyzed by two gas chromatographs (HP 5890), each equipped with two thermal conductivity detectors (TCD) that was controlled by a PC with Chemstation software. The TCDs were kept at 240 °C. During analysis, the columns were heated to 60 – 220 °C using the temperature programming. Each gas chromatograph housed two chromatographic columns, which were: a molecular sieve column for H₂ detection, a 2 ft molecular sieve 5A column for CO detection, a Hayesep Q column (Alltech) for CO₂ and ethylene glycol detection, and a 10 ft Porapak Q column (Alltech) to separate the hydrocarbon products, CO₂, and N₂O. Typically, the first data point was taken 30 minutes after introduction of the feed into the reactor.

2.2.2 Data Analysis

The mass balances and conversions obtained from the GC were calculated using the integrated peak areas for the components of interest. This integration was carried out using the Chemstation software. Prior to the reaction, the reactor was bypassed and a calibration was made to obtain the peak areas for the reactants entering the reactor. The molar concentrations of each species were calculated by dividing the integrated peak areas by the sensitivity factor of that particular gas. The following sensitivity factors were used: O₂ (42), CO₂ (48), CO (42), CH₄ (35.7), N₂O (57.1) and N₂ (42) [5]. The ethylene glycol concentration was determined by its complete combustion into CO₂ over a Pt catalyst.

EG conversions were calculated from conversions to CO and CO₂, and H₂ production efficiency was defined as moles of H₂ produced per mole of EG reacted. The NO and NO₂ concentrations were measured by a NO/NO₂ chemiluminescence analyzer. When the NO_x

analyzer was used downstream, the exit gas stream passed through a Nafion gas sample dryer (Perma Pure Inc.) to remove water vapor for more stable NO_x measurements. All the NO_x conversions reported here are steady state values obtained after at least 1 hr of reaction.

2.3 Catalyst Characterization

2.3.1 Chemisorption Experiments

The amounts of catalyst used for chemisorption measurements ranged from 0.5 – 0.7g. For the chemisorption experiments, trace amounts of O_2 in the H_2 gas were removed by a MnO_2 trap, which was placed right before the reactor. The MnO_2 trap was heated in H_2 at 430 °C for a few hours until it became green prior to the experiments and was regenerated by this treatment when necessary. Downstream of the reactor, a molecular sieve trap was placed to remove any water generated during the reduction. This trap was regenerated after a few experiments. The H_2 uptake was monitored by a TCD, which was kept at 150 °C in a HP 5890 Series II GC. The catalyst sample was placed in a U-tube quartz reactor. Two thermocouples for heating and recording the temperatures were placed on the outside of the reactor at the center of the catalyst bed.

The catalyst sample was first cleaned in 30 mL/min stream containing O_2 at 10 °C/min to 300 °C. After 0.5 hour, the catalyst was purged in 30 mL/min of nitrogen flow for 15 minutes, and reduced in 30 mL/min of H_2 flow for 1 hr at 150 °C. Care was taken to avoid the mixing of oxygen and hydrogen. Then, the catalyst was purged to 450 °C in nitrogen for 1 hr to desorb H_2 , and cooled to room temperature under nitrogen flow before the chemisorption experiments. H_2 chemisorption was performed at room temperature by pulsing 5% H_2/N_2 over a Pt catalyst.

Usually five or more pulses were needed until there was no more H₂ consumption. The chemisorption experiments were performed several times and the results were averaged to calculate the Pt metal dispersion. Calibration was made using the last three pulses. Typically, at least eight pulses were passed over the catalyst sample. Metal dispersions were calculated assuming one H atom adsorbs on one Pt surface atom. The Pt dispersions were 42% for Pt/Al₂O₃ and 46% for Na/Pt/Al₂O₃, as determined by H₂ chemisorption.

The surface area of Pd was measured by the O₂ pulse technique. A 6-way valve with a 1 mL sample loop attached for pulse injections was used. The empty column in the oven was kept at room temperature. The Pd dispersions were 27% for 0.2 wt% Pd/Ti-PILC-B and 40% for 0.1 wt% Pd/Ti-PILC-B, as determined by pulse O₂ (5% O₂ in Helium) chemisorption at room temperature followed by pulse H₂ titration (5% H₂ in N₂) at 100 °C to avoid H₂ absorption by palladium [6]. Before chemisorption, the catalysts were first cleaned in a stream containing O₂ at 300 °C, purged with helium briefly, and then reduced in flowing H₂ at 150 °C and purged with He at 400 °C. A low reduction temperature was used to minimize sintering of Pd under reducing conditions [7]. Metal dispersions were calculated assuming one O atom adsorbs on one Pd surface atom.

2.3.2 X-ray powder diffraction

X-ray diffraction experiments were performed with a Rigaku Powder Diffractometer with Cu K-alpha radiation. The powder samples were packed into a glass sample holder and held in place by pressing the catalyst repeatedly with a glass slide. The tube voltage was increased stepwise to 40 kV and likewise, the current increased to 20 mA. The divergence and scattering

slits were 1° while the focusing slit was $0.3\text{-}0.6^\circ$. A Nickel filter was placed in front of the focusing slit to remove Cu K_β and most of continuous radiation to obtain the pure Cu K_α line. The x-ray diffraction patterns were collected from 10 to 80 (a desired) degrees two theta scan range with a step width of 0.02 or 0.1° and a counting time of 20 or seconds. These were the typical operating parameters used for crystal phase identification. XRD was used to identify the presence of metals, and to determine the incorporation of the Ti into the clay

2.3.3 Surface area measurements

The surface areas of catalysts were determined by N_2 adsorption using the BET method. The catalysts were placed in a sealed tube and attached to the BET system. Before the surface area measurement, the catalysts were heated under vacuum at 250°C until the pressure dropped to 70 mtorr or lower. The catalyst sample tube was then placed in a liquid N_2 filled Dewar flask. Each N_2 molecule was assumed to occupy 0.16 nm^2 .

CHAPTER 3: ETHYLENE GLYCOL REFORMING AS A SOURCE OF REDUCTANTS FOR CATALYTIC NO_x REMOVAL

3.1 Introduction

Recently, there has been a growing interest in using hydrogen as a NO_x reductant for SCR. Not only is H₂ by itself an effective reductant for NO cleanup [1], co-feeding H₂ with hydrocarbons was reported to result in significant improvement in the deNO_x activity at low temperatures [2]. More recently, studies have shown that a mixture of H₂ and CO can effectively remove NO_x in the presence of water and O₂ at temperatures as low as 110 °C [3]. While these reports are encouraging, practically a source of H₂ needs to be secured onboard a vehicle, since there is very little H₂ in the engine exhaust, if any. Therefore, it is necessary to devise an effective means for onboard H₂ delivery.

Although reforming or partial oxidation of diesel fuel might seem to be an obvious onboard source of hydrogen, this method would incur a fuel penalty. Ethylene glycol (EG) is an attractive source of reductant. Unlike alcohols such as methanol and ethanol, it is non-volatile which makes it convenient for transport and safe storage. Since it is used as an antifreeze in automobiles, it has consumer acceptance. One significant advantage of EG compared to fossil fuel as a H₂ source is that EG can be readily and selectively manufactured from sources such as sugars or sorbitol, thus making EG a renewable reductant [4]. This brings about an environmental benefit of using ethylene glycol instead of other non-renewable hydrocarbon sources for diesel exhaust cleanup. Furthermore, this process has been reported to be more energy efficient than the current production of ethylene glycol from petroleum, which is another incentive to utilize ethylene glycol for NO_x removal.

In our scheme, EG reforming would take place in a separate unit. The H₂ and CO produced would then be injected into the engine exhaust, and the mixture will be passed over a catalytic deNO_x unit. Reforming of EG in the aqueous phase has been reported by Dumesic and coworkers, who showed that Pt/Al₂O₃ catalysts are highly active and selective for this reaction [5]. Their process was, however, targeted for the production of H₂ for fuel cell applications [6] and was carried out at elevated pressures of at least 2.9 MPa [7]. For our purpose of diesel exhaust cleanup, low concentrations of hydrogen are needed, of the order of a few thousand parts per million [8]. Thus, gas-phase EG reforming at atmospheric pressure would be more desirable because of simpler equipment.

First, the feasibility of such an ethylene glycol-deNO_x (EG-NO_x) system needs to be evaluated. Specifically, both the volume of catalyst and the amount of ethylene glycol required on board to meet the stipulated NO_x standard were estimated based on relevant literature information. For the reforming of ethylene glycol, one mole of C₂H₆O₂ can produce up to 5 moles of H₂ and 2 moles of CO₂ as shown by Eqn. 3.1.



Under the conditions at which EG reforming was conducted, Shabaker et al. observed low levels of CO in the effluent due to concomitant water-gas shift [9]. Concentrations of carbon containing products, other than CO_x, were found to be exceptionally low. The further the water-gas shift reaction proceeds, the more H₂ is formed and the less the amount of CO remaining. Regardless of the extent to which this reaction proceeds, one mole of ethylene glycol reformed

will always yield a total of 5 moles of H₂ and CO. More concerning the effect of CO on the subsequent deNO_x reaction will be discussed in Chapters 4 and 5.

Using H₂ as the reductant, the NO_x reduction efficiency can be approximated based on data for one of the best performing catalysts reported in the literature. For a simulated feed containing 500 ppm NO, 1000 ppm CO, 3000 ppm H₂, 5% H₂O, and 5 % O₂ over a 0.5 wt% Pd catalyst supported on a titanium-aluminum mixed oxide, 94% NO_x conversion was reached at 165 °C [8]. Since both H₂ and CO are completely consumed under these conditions, this would translate to 8 moles of reductants required to convert 1 mole of NO. Therefore, 10% efficiency for NO_x reduction by H₂ was used in our calculation.

One way to carry out the evaluation is to assume that 600,000 L/h of exhaust gas containing 500 ppm of NO_x needs to be cleaned. This is equivalent to 0.21 moles NO/min. For 10% efficiency in NO_x reduction using H₂ and formation of 5 moles of H₂ per mole of C₂H₆O₂ reformed, 0.42 moles of C₂H₆O₂/min or 1.4 L/h of C₂H₆O₂ is needed. At 225 °C, with a 5 wt% ethylene glycol solution, the rate of H₂ production was reported by the group of Dumesic to be 450 μmol/cm³ cat.-min over a Pt/Al₂O₃ catalyst [9]. Using 450 μmol/cm³ cat.-min for the reforming rate, the volume of catalyst needed to generate the required H₂ would be 1000 cc. Therefore, both the volume of the reforming catalyst and the volume of ethylene glycol required are manageable for practical integration into the design of a vehicle. In relation to the reforming rate, one of the goals of this study is to achieve a reforming rate that is considerably higher than that reported for aqueous phase reforming of ethylene glycol.

This chapter describes the results of the study of gas-phase reforming of ethylene glycol at atmospheric pressure to produce H_2 for lean NO_x reduction. Specifically, the efficiency of H_2 production as a function of feed composition at 230 °C was examined. This temperature was found to be optimal for gas-phase EG reforming to H_2 in preliminary experiments. Since the sole purpose of EG reforming to H_2 is for NO_x cleanup for automotive application, it is important to examine the efficiency with which H_2 is produced. During this study, it was observed that deactivation of the Pt/Al_2O_3 catalyst could be avoided by the addition of oxygen to the reforming mixture. The effect of Pt/Al_2O_3 catalyst modification with Na ions was also investigated.

3.2 Experimental

3.2.1 Catalyst

The $Pt/\gamma-Al_2O_3$ and $Na/Pt/\gamma-Al_2O_3$ catalysts used in this study were prepared according to the procedure described in section 2.1. Both catalysts contained 1 wt% Pt with the Na modified $Pt/\gamma-Al_2O_3$ catalyst containing 1.4 wt% Na. Most of the reforming studies were carried out using the $Na/Pt/\gamma-Al_2O_3$ catalyst, and the results reported in this chapter correspond to this sample unless otherwise stated. Examination of these catalysts by H_2 chemisorption showed the Pt dispersions to be 42% for Pt/Al_2O_3 and 46% for $Na/Pt/Al_2O_3$.

3.2.2 Reaction Studies

Reaction studies were conducted according to the procedure described in section 2.2. Regeneration of a reaction-deactivated catalyst was carried out after the catalyst had lost approximately 37% of its initial activity, which resulted after about 5 hr time-on-stream. At this

point, the reforming catalyst was exposed to flowing N_2 at a flow rate of 100 mL/min for 60 minutes. Alternatively, a N_2 stream containing water was used to regenerate the catalyst. This was accomplished by passing the N_2 through a water saturator at room temperature. Its vapor pressure was assumed to correspond to saturation of the stream (1.5% of an atmosphere). After the regeneration procedure with water, the system was purged with N_2 , and the EG reforming reaction was carried out to determine the catalyst activity.

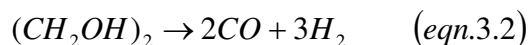
3.3 Results and Discussion

The catalyst used for the ethylene glycol reforming reaction was a Pt supported on a large pore γ - Al_2O_3 catalyst. Pore structure can influence supported metal catalysts in two ways. Supports, as porous materials, can affect the manner in which the dispersed metallic particles are deposited as well as reactant access to the active site. A support with a large pore structure would allow better access of reactant to the active metal and could possibly alleviate deactivation due to pore plugging, which blocks access of reactants to the active sites located in the pores.

The Na/Pt/ Al_2O_3 catalyst is an effective catalyst for EG reforming. Close to 100% EG conversion to H_2 was reached over this catalyst when reforming was conducted with 410 ppm EG, indicating that reactions between CO/ CO_2 and H_2 such as the methanation and Fischer-Tropsch reaction, do not occur to any significant extent under these reaction conditions.

3.3.1 Effect of O₂ Concentration in EG Reforming.

A series of preliminary experiments was conducted to identify conditions suitable for gas phase EG reforming. At 230 °C, with an EG concentration of 410 ppm in the feed and in the absence of O₂, a steady production of H₂ of about 1200 ppm was observed as shown by Fig. 3.1. This is equivalent to about 3 mol H₂ produced per mole of EG consumed, or a H₂ production efficiency of 3. Within experimental error, the pseudo-steady state CO produced remained unchanged at a value of 730 ppm. Thus, the H₂/CO formed was calculated to be 1.6. A H₂/CO ratio of 1.6 and a H₂ production efficiency of 3 are both indicative of the EG decomposition reaction (Eqn. 3.2).



The high level of CO detected in the product stream of the reforming unit suggests that water-gas shift may not be an important aspect of gas phase EG reforming under the current reaction conditions. In relation to that, it is pertinent to note the drop in CO₂ production from an initial value of approximately 190 ppm down to 90 ppm after 2 hr time-on-stream, which further decreases to a pseudo-steady state value of about 20 ppm after 12 hr. Alkane formation was insignificant over the Na/Pt/γ-Al₂O₃ catalyst under our reaction conditions, similar to that observed for aqueous phase EG reforming [10].

C₂ compounds such as ethane were not detected in the effluent (only small amounts of methane were detected). This indicates that the Pt catalyst has high catalytic activity for breaking C–C bonds. Dumesic and co-workers concluded that C–C bond cleavage is a fast step

for ethylene glycol reforming after it was found that the rate of hydrogen production for aqueous-phase reforming of methanol was similar to that of ethylene glycol over Pt/Al₂O₃ [11].

Having identified conditions under which steady production of H₂ occurs, the next task was to carry out reforming at higher EG concentrations to generate sufficient H₂ for effective NO_x removal downstream. Increasing the EG concentration to 2.2% caused catalyst deactivation, although a concentration of H₂ higher than 1.5% could be obtained initially (Fig. 3.2). The corresponding EG conversion under these reaction conditions is about 25%. Within experimental error, the H₂ production remained at a pseudo-steady state value of about 1.2% after 100 minutes time-on-stream.

It was found that deactivation could be prevented by adding O₂ in the feed at rates equivalent to O₂/EG ratios higher than 0.7. These data are summarized in Table 3.1, where it is shown that over the range of O₂/EG from 0.7 to 1.5, H₂ was produced with an efficiency of 1.6 ± 0.2. These efficiency values were lower compared to runs without O₂. The hypothesis is that the higher EG conversion and lower H₂ production efficiency (implying more water formation) in the presence of O₂ resulted in heating of the catalyst bed, such that condensation of EG in catalyst pores no longer occurred. Oxygen concentrations also affected the EG conversion in the following manner: the EG conversion was higher for higher O₂ concentrations (compare runs 6 and 9 versus runs 7 and 8) and for lower EG concentrations (compare runs 1, 2, and 5).

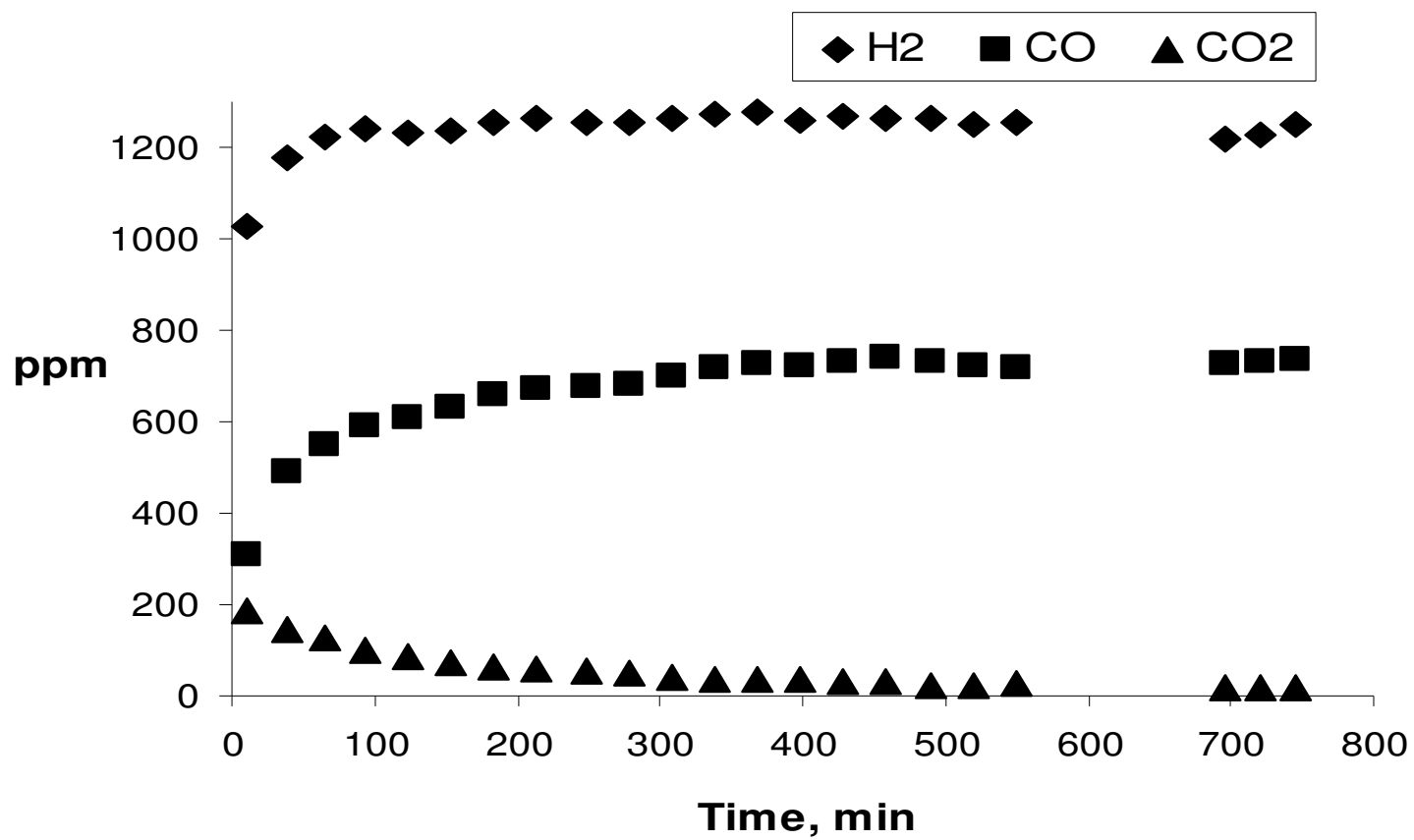


Figure 3.1. Ethylene glycol reforming over 0.1 g Na/Pt/Al₂O₃ at 230 °C as a function of time-on-stream. Feed: 410 ppm EG, 0.37% H₂O, balance N₂, total flow rate 107 mL/min.

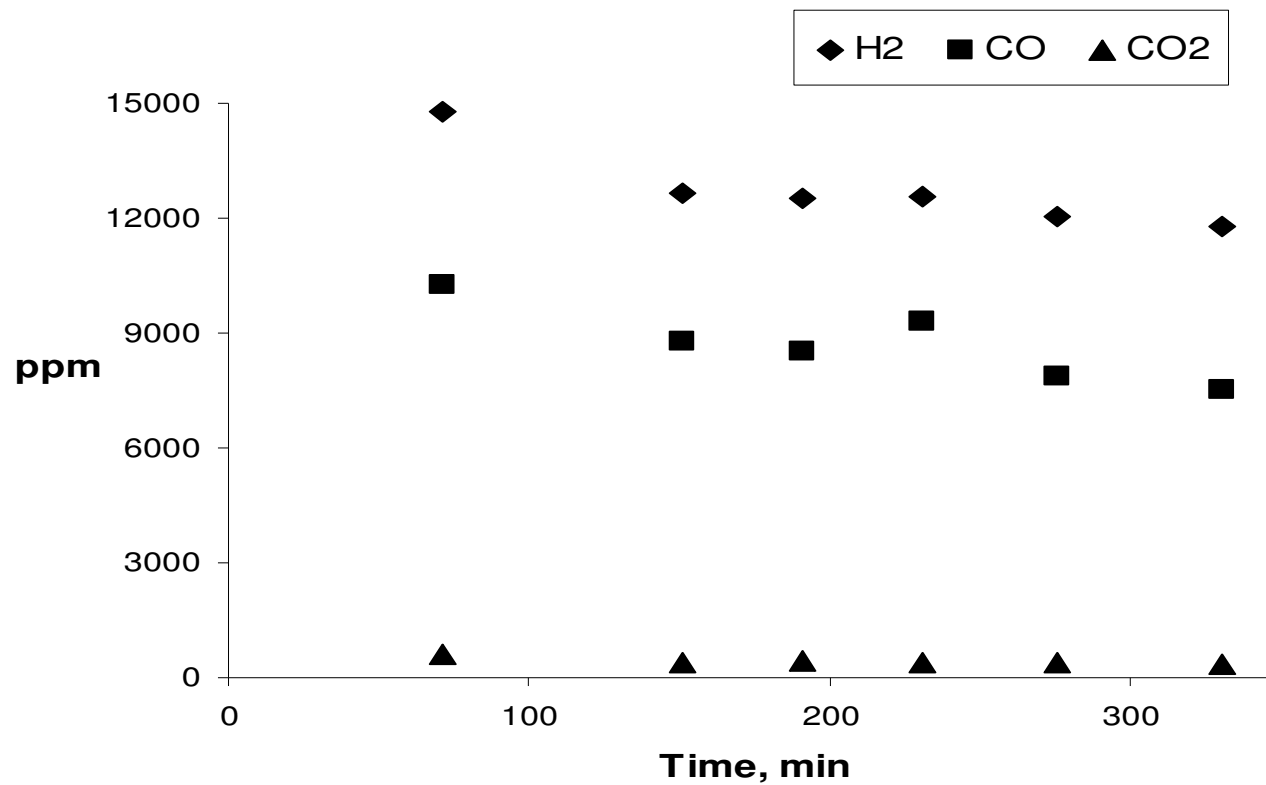


Figure 3.2. Ethylene glycol reforming over 0.1 g Na/Pt/Al₂O₃ at 230 °C as a function of time-on-stream. Feed: 2.2% EG, 27.5% H₂O, balance N₂, total flow rate 46 mL/min.

Table 3.1. Oxidative reforming of EG at 230 °C over 0.1 g Na/Pt/Al₂O₃. Total flow rate 47–49 mL/min.

Run	1	2	3	4	5	6	7	8	9
EG in feed (%) ± 0.2	4.1	2.2	2.8	3.8	2.7	3.1	3.0	3.0	3.2
Water in feed (%) ± 1.9	25.2	26.6	26.2	23.9	25.5	19.5	18.7	18.5	19.8
O ₂ in feed (%) ± 0.1	2.9	3.2	2.3	3.8	2.8	3.8	4.5	4.7	3.6
EG conversion (%) ± 3	65	95	69	87	70	69	89	83	76
CO in product (%) ± 0.02	0.8	0.4	0.8	1.6	0.7	0.7	0.6	0.5	0.9
CO ₂ in product (%) ± 0.13	4.5	3.7	2.6	5.1	3.2	3.6	4.8	4.5	3.9
CO/CO ₂ ± 0.01	0.2	0.1	0.3	0.3	0.2	0.2	0.1	0.1	0.2
H ₂ in product (%) ± 0.2	5.3	4.0	3.4	6.3	4.3	4.0	4.3	3.4	4.5
H ₂ formed/EG in feed ± 0.1	1.3	1.8	1.2	1.6	1.6	1.3	1.4	1.1	1.4
O ₂ in feed /EG in feed ± 0.1	0.7	1.5	0.8	1.0	1.0	1.2	1.5	1.6	1.1

The data in Table 3.1 also show that with 3.8% EG in the feed, a H₂ concentration as high as 6.3% could be obtained in the product stream of 49 mL/min. This would produce a H₂ concentration of over 4000 ppm when injected into an exhaust stream of about 500 mL/min, which is within the range sufficient for effective NO_x reduction in a practical exhaust [3].

In addition to achieving a stable H₂ production, O₂ in the feed could also provide control of the H₂ to CO ratio in the product stream. Over the range of conditions tested in Table 3.1, the CO/H₂ ratio ranged from about 1/4 to 1/10. It is possible to eliminate CO from the product stream by operating at an O₂ to EG ratio of 2 in a feed mixture containing 6900 ppm EG, 4.3% H₂O at a total flow rate of 142 mL/min using 1.0 g Na/Pt/Al₂O₃. Under these reaction conditions, a H₂ efficiency of 1.7 is obtained. Having the capacity to control the H₂ to CO ratio in the effluent is advantageous for NO_x reduction, since the efficiency of supported Pd catalysts has

been reported to depend on the CO/H₂ reductant ratio [3]. More of this will be discussed in Chapter 5.

Practically, operating ethylene glycol reforming under oxidative conditions is beneficial because the exothermic nature of the oxidation reaction offsets the energy required for the reforming reaction. Consequently, the energy demands for the overall reaction are reduced.

3.3.2 Effect of EG Concentration on H₂ Production

The effect of EG concentration on reforming to H₂ was investigated and shown in Table 3.2. For each of these experiments, the O₂/EG and H₂O/EG ratios in the feed mixture were maintained at a constant value of 1.0 and 6.2 respectively. An O₂ to EG ratio of 1.0 was selected since it was previously found that this O₂ concentration is adequate to prevent deactivation as well as sustain a sufficiently high H₂ production efficiency.

These results show that increasing the ethylene glycol feed concentration from 3.5 to 8.2% did not have a significant impact on the H₂ production efficiency. Shabaker et al. reported that increasing the concentration of ethylene glycol for aqueous phase reforming did not affect the selectivity to H₂ significantly, similar to our observation for gas phase EG reforming [9]. The production of methane increased slightly as the EG concentration increased to 8.2%. Alkane formation is undesirable since the formation of alkanes consumes H₂, leading to a reduction in the H₂ production efficiency. For our application, the methane formed is considered unproductive since it is not an effective reductant for low temperature NO_x reduction. With this in view, it would be beneficial to conduct reforming at EG feed concentrations below 5%.

Table 3.2. Effect of EG concentration in EG reforming at 230 °C.

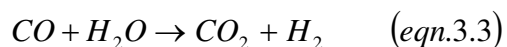
Feed EG (%) ±0.2	H ₂ formed/EG in feed ±0.1	CH ₄ formed/EG in feed ±0.01	EG conversion (%) ±3	CO/CO ₂ formed ±0.01
3.5	1.9	0.05	71	0.3
5.0	1.8	0.05	68	0.3
8.2	1.7	0.08	68	0.6

Reaction conditions: 0.05 g catalyst; 230 °C; O₂/EG =1.0, H₂O/EG = 6.2, balance N₂, total flow rate 30-49 mL/min.

3.3.3 Effect of Water Concentration on H₂ Production

The effect of H₂O concentration in the feed on oxidative reforming was investigated, and the results are shown in Table 3.3. For the same EG concentration, H₂ production efficiency increased with increasing H₂O concentration. However, unlike O₂, increasing the water content had little effect on the EG conversion. As one might expect, the reaction of H₂O with EG is not as facile as the oxidation of EG. As a result, changes in the H₂O concentration showed less impact on the EG conversion than O₂ concentration.

Increasing the H₂O concentration increased the H₂/CO ratio, which could be due to increasing contribution from the steam reforming reaction (Eqn. 3.1). Alternatively, it could also be the result of the water-gas shift (WGS) reaction (Eqn. 3.3). Using the exit CO and CO₂ concentrations in Table 3.3, the H₂/H₂O ratios were calculated to determine if WGS equilibrium were attained, and found that these calculated ratios were substantially higher than the experimental values. Thus, under our conditions, the reaction mixture was far from the WGS equilibrium.



To acquire a more precise assessment of the degree to which water influences H₂ formation, two additional experiments were conducted for which the difference in the water content of the feed mixture was more extreme. From these experiments, it was determined that a 60% increase in H₂ production can be obtained when the H₂O concentration is 25.4% versus when no H₂O was present.

Table 3.3. Effect of H₂O concentration in EG reforming at 230 °C.^a

Feed EG (%) ±0.2	Feed H ₂ O (%) ±1.8	H ₂ (%) ±0.1	H ₂ /H ₂ O ±0.01	CO ₂ (%) ±0.24	EG conv. (%) ±3	H ₂ /H ₂ O ^b ±1.1
3.6	44.8	6.1	0.1	4.5	75	27
3.8	23.9	5.3	0.2	4.5	70	26
3.9	17.9	5.1	0.3	4.2	75	28
2.0	0	1.0	-	2.4	62	-
2.0	25.4	1.6	0.1	2.6	69	11

^a Reaction conditions: (1) for 3.6 to 3.9% EG feed: 3.7±0.1% O₂, balance N₂, total flow rate 46–70 mL/min, 0.1 g Na/Pt/Al₂O₃; (2) for 2.0% EG feed: 2.5% O₂, balance N₂, total flow rate 57 mL/min, 0.05 g Na/Pt/Al₂O₃.

^b Calculated using measured CO and CO₂ values, and K (at 500 K) = 134.1.

Whether our catalysts could catalyze the WGS reaction readily was examined, and the results are shown in Table 3.4. Both the experimental product ratios and the equilibrium ratios calculated from the feed are presented. In the absence of O₂ in the feed, the composition of the product stream was substantially different from the equilibrium composition, suggesting that the

WGS reaction was relatively slow under our conditions. When O₂ was introduced in the feed, it reacted readily with CO, but did not completely consume CO to form CO₂.

This effect of O₂ was also observed during EG reforming: there was less CO in the product stream in experiments with higher O₂ concentrations. The effect on H₂ production was more complicated. Oxygen first increased the H₂ production, probably due to higher CO₂ concentration, and then decreased it when H₂ oxidation became more significant. In all cases, however, the H₂ formed was far from the predicted value for WGS equilibrium. Thus, during EG reforming, H₂ was produced primarily from the reforming reaction, and the contribution from WGS was minor. These data also showed that H₂ oxidation was slow, such that the addition of O₂ did not result in a significant reduction in H₂ production.

Table 3.4. WGS reaction over 0.1 g Na/Pt/Al₂O₃ at 230 °C.

O ₂ (%) ±0.02	Product concentrations			Calculated equilibrium concentrations		
	H ₂ (%) ±0.01	CO ₂ (%) ±0.03	CO (%) ±0.06	H ₂ * (%)	CO ₂ * (%)	CO* (%)
0	0.19	0.19	1.6	1.78	1.78	0.0010
0.44	0.34	0.74	1.1	0.90	1.78	0.0005
0.86	0.14	0.75	1.1	0.02	1.74	0.00001

Feed: 1.76 ± 0.06% CO, 25 ± 1% H₂O, total flow rate 90 ± 2 mL/min.

As mentioned earlier, in the absence of O_2 , the H_2 production efficiency approached 3. In the presence of O_2 , the efficiency was reduced to 1.3 – 1.6. One way to achieve higher H_2 production efficiency is to enhance the WGS activity of the reforming catalyst. In this respect, the Pt catalyst was modified with ceria (8.3 wt% Ce loading) according to the procedure described in Section 2.1. Selection of ceria was based on literature reports of its role in promoting the WGS reaction. While Pt supported on nanocrystalline ceria (Pt/CeO₂) is one of the best performing low-temperature WGS catalyst [12], the Pt/CeO₂ catalyst deactivated during aqueous-phase reforming of ethylene glycol [5].

To obtain the WGS activity of Pt/CeO₂ catalyst while retaining the EG reforming activity, the amount of ceria added to the alumina was designed to be less than a monolayer so that the final support would still have alumina exposed on its surface. Prior to modifying the existing Na/Pt/Al₂O₃ catalyst with ceria, Pt/CeO₂ was first prepared and tested for its WGS activity. The results for WGS with different O_2 concentrations using the Pt/CeO₂ catalyst are listed in Table 3.5. The Pt/CeO₂ catalyst is an excellent WGS catalyst at the reforming temperature. However, as the amount of O_2 added to the WGS feed increased, there was a corresponding decrease in the H_2 produced.

Table 3.5. WGS reaction over 0.1 g Pt/CeO₂ at 230 °C

O ₂ (%) ±0.02	H ₂ (%) ±0.01
0	1.30
0.34	0.70
0.45	0.30
0.90	0

Feed: 1.38-1.44% CO, 39-41% H₂O, total flow rate 110 mL/min.

After testing of the Pt/CeO₂ catalyst for its WGS activity, ceria was incorporated to the alumina, forming a Ce-Al₂O₃ mixed support before impregnation of Pt and Na. The results for EG reforming with the Na/Pt/Ce-Al₂O₃ catalyst are shown in Table 3.6. Although modification of the reforming catalyst with ceria did not bring about the anticipated increase in the H₂ productivity efficiency, deactivation was not observed over the duration of reforming. In the case where the Na/Pt/Ce-Al₂O₃ was used, an ethylene glycol conversion of 66% was observed, compared to a conversion of 87% when Na/Pt/Al₂O₃ was used. This difference suggests that the reforming activity is dependent on the support used. Regarding this, there is supporting evidence in the literature suggesting that selectivity towards alkane formation is dependent on the nature of the support to a greater extent than on the Pt metal dispersion [11]. Alkane formation uses up hydrogen, thereby decreasing the resultant hydrogen obtained.

Table 3.6. Oxidative Reforming of EG at 230 °C over 0.1 g catalyst.

Catalyst	Na/Pt/Ce-Al ₂ O ₃	Na/Pt/Al ₂ O ₃
EG conversion (%) ± 3	66	87
CO in product (%) ± 0.02	1.4	1.6
CO ₂ in product (%) ± 0.13	3.7	5.1
CO/CO ₂ ± 0.01	0.4	0.3
H ₂ in product (%) ± 0.2	4.4	6.3
H ₂ production efficiency ± 0.1	1.8	1.9

Feed: $3.8 \pm 0.1\%$ O₂, $23.9 \pm 1.9\%$ H₂O, $3.8 \pm 0.2\%$ EG, balance N₂, total flow rate 51 mL/min.

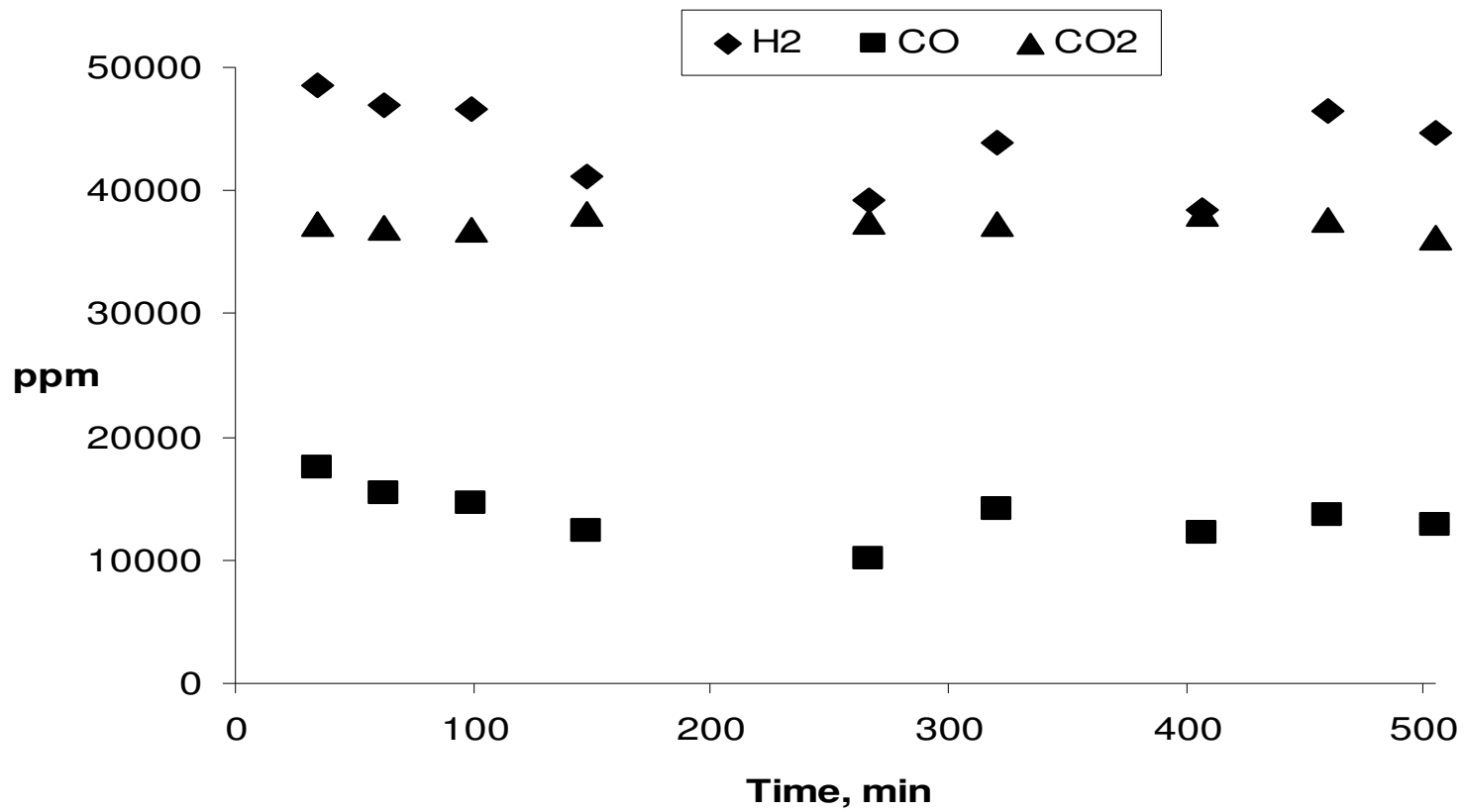


Figure 3.3. Ethylene glycol reforming over 0.1 g Na/Pt/CeO₂-Al₂O₃ at 230 °C as a function of time-on-stream. Feed: 3.84% EG, 23.9% H₂O, 3.8% O₂, balance N₂, total flow rate 51 mL/min.

3.3.4 Effect of Na Modification of Pt/Al₂O₃

For the reforming reaction, the role of an alkali promoter, such as sodium (Na) is complex. Potentially, it could neutralize the surface acidity to minimize coking over the catalyst [13]. It could also catalyze the reaction between water vapor and carbon containing products from the decomposition of the hydrocarbon that is being reformed. In numerous systems the alkali acts by enhancing the adsorption of a particular reactant and/or by promoting the rate of its dissociation [14, 15].

Pt/Al₂O₃ catalysts can be deactivated by ethylene glycol reforming. For EG reforming at an EG concentration of 410 ppm over a Pt/Al₂O₃ catalyst, deactivation is observed as the reaction proceeds as illustrated by Fig. 3.3. A gradual decrease from an initial H₂ production of 790 ppm to a pseudo-steady state H₂ production of approximately 500 ppm occur over 5hr of reaction. The decrease in H₂ production is accompanied by a corresponding decrease in ethylene glycol conversion to carbon dioxide. The amount of carbon dioxide produced begins with an initial value of 245 ppm to 15 ppm after 5 hr of reaction.

Interestingly, the activity could be restored by purging the catalyst in a stream of nitrogen for 1 hr at the reaction temperature of 230 °C. Regeneration was more effective when the nitrogen stream was saturated with water. Results from these regeneration studies suggest that deactivation was not due to sintering of Pt particles or coking. Since the catalysts had been subjected to 260 °C calcination during preparation, it is unlikely that the reaction temperature of 230 °C would cause significant sintering of the Pt particles. Moreover, it is not likely that

treatment in nitrogen at 230 °C could result in redispersion of the hypothetically sintered Pt particles to their initial form.

The regeneration results also suggest that the deactivation was not due to formation of a higher molecular weight polymer or other carbonaceous species, since it would not be expected that treatment in nitrogen at 230 °C would regenerate a catalyst deactivated by carbon deposition. Consequently, loss of activity is likely due to condensation of EG or small oligomers formed from it in the catalyst pores that could be removed by nitrogen purging, thus allowing access of reactants to metal particles inside these pores.

Another possibility for deactivation is due to CO poisoning of the Pt catalysts [16]. Carbon monoxide which is a major product in this reforming reaction is known to adsorb strongly on Pt surfaces, to the extent of suppressing O₂ adsorption in CO oxidation [17]. One way by which removal of CO from the catalyst surface could take place is by its reaction with H₂O via the water-gas shift reaction to form weakly bound CO₂ species that readily desorb from the Pt surface. However, the experimental data shows low concentration of CO₂ formation indicating that the water-gas shift reaction is not occurring at an appreciable rate. For our reaction, it is doubtful that deactivation is caused by CO poisoning. Temperature programmed CO desorption (CO-TPD) measurements for a Pt/Al₂O₃ catalyst showed CO desorption occurred at 332 °C [18]. Since the initial activity of our catalyst is recovered by purging in nitrogen at 230 °C, that is 100 °C lower than the temperature required to desorb CO from Pt, the decrease in reforming activity does not stem from strongly held CO on Pt particles.

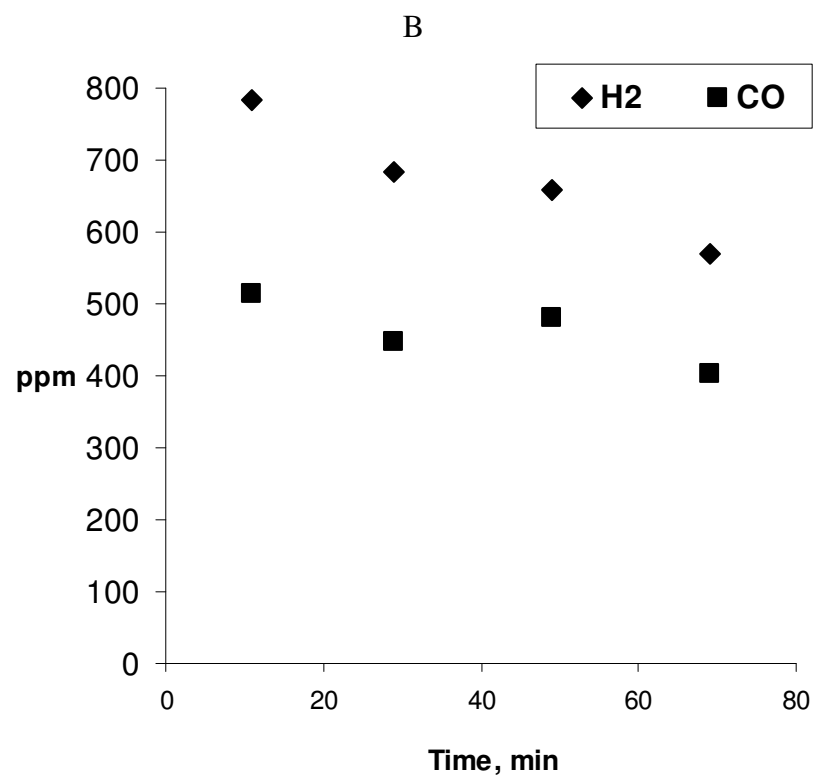
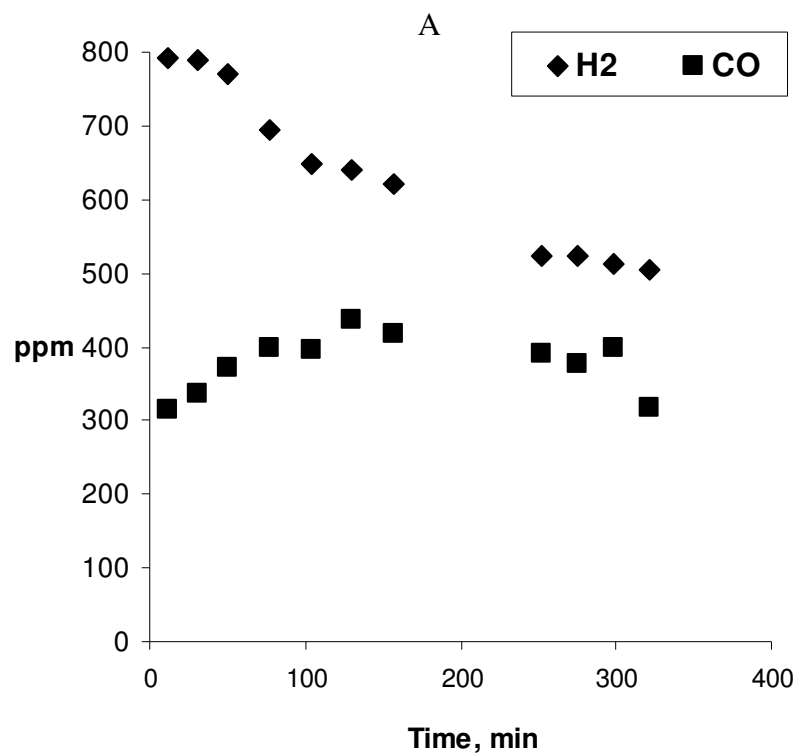


Figure 3.4. Ethylene glycol reforming over 0.1 g Pt/Al₂O₃ at 230 °C as a function of time-on-stream. Feed: 410 ppm EG, 0.37% H₂O, balance N₂, total flow rate 107 mL/min. Figure 3.3B: Deactivated catalyst after purging in nitrogen

Sustained delivery of H₂ from gas phase ethylene glycol reforming for NO_x cleanup was achieved by modification to the reforming catalyst. Under identical reaction conditions, but with a Pt catalyst that is promoted with Na, deactivation did not occur over a span of over 12 hr of reforming (refer to Fig. 3.1).

Table 3.7 compares the EG reforming activities of Pt/Al₂O₃ with and without modification by Na carbonate. For these reactions, reforming was performed at an EG concentration of 2% with 2.5% O₂ added to the reformat. Na modification enhanced the activity of the catalyst. From H₂ chemisorption experiments, the dispersions of Pt/Al₂O₃ and Na/Pt/Al₂O₃ were determined to be 42% and 46%, respectively. Thus, the different activities were not due to different dispersions.

Table 3.7: Effect of Na Modification of Pt/Al₂O₃ in EG Reforming

Catalysts	H ₂ formed (%) ±0.1	EG conv. (%) ±3.5	CO formed (%) ±0.01	CO ₂ formed (%) ±0.1
Na-Pt/Alumina	2.6	84	0.2	3.2
Pt/Alumina	1.6	69	0.2	2.6

Reaction conditions: 0.05 g catalyst; 230 °C; 2.0% EG, 2.5% O₂, 25.4% H₂O, balance N₂, total flow rate 57 mL/min.

The effect of Na modification had been observed in other systems involving CO [19]. In the reaction of propene and CO reduction of NO over Pt/Al₂O₃ in the presence of oxygen, a promotional effect of Na was observed for both CO and propene oxidation and NO reduction. The authors determined that the improved activity was not due to Na changing the Pt dispersion, similar to the observation here. Rather, the principal effect was attributed to the modification of Pt surface chemistry by Na. It is possible that addition of basic compounds, such as Na₂O, results in transfer of electron density from Na₂O to Pt. Consequently, the more electron rich Pt reduces the extent of σ -bonding of CO, thus weakening its binding to Pt, causing the catalyst to be more active for the EG reaction. There is evidence in the literature indicating weaker adsorption of CO due to alkali promotion [20]. Investigation of the effect of Na on the CO adsorption by infrared spectroscopy showed a decrease in CO adsorbance with increasing Na₂O content [21]. Na is known to inhibit excessive adsorption of hydrocarbon [22].

Na modification affects the water-gas shift activity of the reforming catalyst. A higher ratio of CO₂/CO was observed in the product for the Na/Pt/Al₂O₃ catalyst, as well as a higher H₂ production efficiency. These can be explained as this catalyst is more active for the water-gas shift reaction than the unmodified Pt/Al₂O₃. Our results are in agreement with that of Lee et al., who reported that the addition of basic components such as K₂O and Na₂O to Pt/Al₂O₃ significantly enhanced the water-gas shift reaction [23].

Alkali modification of the adsorption strength of the reactants and consequently the relative coverage of the various reactants on supported Pt catalysts, have been shown in numerous systems relevant to ours. However, the increase in activity observed here cannot be

assigned exclusively to Na modification to Pt, without information on the Na distribution between the Pt metal and the Al_2O_3 support. For the reaction between CO and NO over platinum, it was shown that sodium electrochemically supplied to the surface of a porous Pt film produced large increases in both the activity and N_2 selectivity [24]. The response to alkali promotion is exactly the same, in terms of both the activity and selectivity as when the reaction was performed with a supported catalyst modified with sodium. In the case of the electrochemically promoted (EP) catalyst, there is no question that this observation is due to alkali that resides on the surface of the metal film [25]. Therefore, it is reasonably certain that for our EG system promotion is principally due to the effect of Na on the active metal component, rather than on the support.

3.5 Conclusion

We have demonstrated the feasibility of gas-phase EG reforming to generate H_2 at concentrations suitable for lean NO_x removal. Stable production of H_2 could be obtained with the inclusion of O_2 to the feed. For EG reforming carried out with 3.8% EG, the rate of H_2 production was $670 \mu\text{mol}/\text{cm}^3 \text{ cat.}\cdot\text{min}$ over the $\text{Na}/\text{Pt}/\text{Al}_2\text{O}_3$ catalyst (refer to Table 3.1). The EG conversion, H_2 production efficiency, and H_2/CO ratio depend on the O_2 and H_2O concentrations in the feed. Other than the influence of the reaction conditions on the yields from the system, modification of the $\text{Pt}/\text{Al}_2\text{O}_3$ catalyst with Na improved H_2 production. Under the present EG reforming conditions, it was determined that water-gas shift is not a principal pathway for H_2 production.

CHAPTER 4: PARAMETER CONTROLLING ACTIVITY OF Pd CATALYSTS FOR H₂ - SELECTIVE CATALYTIC REDUCTION OF NO_x

4.1 Introduction

Supported Pd catalysts were recently reported to be highly active for hydrogen reduction of NO_x with high N₂ selectivity at temperatures around 140 °C [1]. More interestingly, these catalysts not only sustain a high NO reduction in the presence of CO, but achieves a higher NO reduction when both H₂ and CO is present. This aspect of Pd catalyst is quite different compared to Pt catalysts. Although supported Pt catalysts have comparable NO reduction activity when hydrogen is used as the reductant, the NO conversion drops from 90% to less than 5% as soon as 250 ppm of CO is added to the reaction feed [2].

Considering this distinct characteristic of the Pd catalyst, it is worthwhile to conduct further studies of this catalyst for NO reduction using a H₂-CO mixture since CO is generally found in the diesel exhaust. Two of the best performing catalysts for H₂-CO selective catalytic reduction (SCR) of NO are a Pd supported on a titanium-aluminum mixed oxide (Pd/TiO₂-Al₂O₃) and a Pd supported on titania pillared clay (Pd/Ti-PILC). As for the origin of the activity, some have proposed that the NO_x reduction activity of Pd catalysts is dependent on the support [3]. In a feed containing 3500 ppm H₂, 500 ppm CO, 500 ppm NO, 5% O₂, and a W/F of 0.03 gs/mL, NO conversion at 150 °C was close to 100% for Pd/TiO₂-Al₂O₃ versus a conversion of 38% for Pd/TiO₂ and 12% for Pd/Al₂O₃. [4].

The group of Lambert used a combination of in-situ DRIFTS, XPS, HREM and reaction studies to elucidate the difference in activity on the various supports. Based on the results obtained from the in-situ DRIFTS studies, a reaction mechanism involving CO reaction with NO

to form isocyanate (NCO) species was proposed. Hydrolysis of NCO leads to the subsequent formation of ammonia (NH_3). The ammonia that is generated in-situ reduces NO to nitrogen. The higher activity of Pd/ TiO_2 - Al_2O_3 was ascribed to the synergistic effect between TiO_2 and Al_2O_3 . Pd on TiO_2 can generate Pd-NCO species more efficiently than Pd on Al_2O_3 . The NCO then spills over to the support. While NCO on TiO_2 is not stable in the presence of oxygen, on alumina, the NCO is hydrolyzed to NH_3 [5]. Therefore, a TiO_2 - Al_2O_3 mixed support with an optimal TiO_2 to Al_2O_3 ratio promotes the generation and stabilization of key reaction intermediates, ultimately leading to an exceptionally high NO_x conversion in the low temperature region.

Meanwhile, other than the catalyst support, others have suggested that the Pd precursor can have a tremendous effect on the NO_x reduction activity [2]. In a feed containing 3500 ppm H_2 , 500 ppm CO, 500 ppm NO, 5% O_2 , and a W/F equivalent to 0.03 gs/mL, NO conversion at 150 °C was 90% for a Pd/ Al_2O_3 catalyst prepared using a Pd chloride precursor versus a conversion of 12% for a Pd/ Al_2O_3 catalyst prepared using a Pd nitrate precursor. The origin of this variation in NO conversion due to different Pd precursors is not well understood. The wide variation in the activities of catalysts with similar compositions cannot be explained by the existing models depicting the active centers.

The goal of this study is to determine the origin of the high activity of Pd catalysts for H_2 reduction of NO under oxidizing conditions. This information could potentially facilitate preparation of even more active catalysts for lean NO reduction. After careful assessment of the existing literature results, our hypothesis is that the Pd particle size is a key parameter controlling the NO_x reduction activity. For our study, Pd supported on titania-pillared clay was selected due

to its high activity as well as high selectivity to N_2 [6]. Practically, having titania as a component of the catalyst is advantageous since it is tolerant to low concentrations of sulfur that is found in diesel exhaust [7]. The formation and accumulation of sulfate compounds on the catalysts often leads to irreversible poisoning of the catalyst.

The effects of Pd particle size were investigated by varying the Pd weight loading over the Pd/Ti-PILC catalysts. During the characterization of the Pd/Ti-PILC catalysts by H_2 chemisorption, anomalous behavior was observed which will also be discussed. Since water vapor is one of the main components of diesel exhaust, the effect of water on NO conversion was also examined. The result from these studies is described in this chapter.

4.2 Experimental

4.2.1 Catalyst

The Pd/Ti-PILC catalysts used in the reaction studies were prepared as described in section 2.1. Two batches of Ti-PILC prepared with different amounts of Ti were used. To the batch of pillared clay denoted by Ti-PILC-A, the amount of Ti precursor added was such that the composition of titania in the final catalyst is equivalent to 49 wt%, while for Ti-PILC-B that amount is equivalent to 39 wt%. A batch of catalysts of 0.1, 0.2 and 0.5 wt% Pd loading was prepared with Ti-PILC-B, and another batch of 0.1 wt% Pd was prepared with Ti-PILC-A. The chemical compositions of the starting clay and the Ti-PILC-B samples as determined by XRF are listed in Table 4.1.

Table 4.1

Chemical Compositions of Bentonite and Ti-PILC determined by XRF.

Oxides (wt%)	Bentonite	Ti-PILC-B
SiO ₂	69.5	42.0
TiO ₂	0.1	39.4
Al ₂ O ₃	20.3	12.9
Fe ₂ O ₃	3.7	3.2
MgO	2.5	1.3
K ₂ O	0.4	0.2
Na ₂ O	2.6	0
CaO	1.0	0.2

The loss of Na₂O upon pillaring is an indication that successful intercalation of Ti has taken place since intercalation occurs by the exchange of the Na cations located between the layers by the Ti polycations. Indeed, it is found that whenever the XRF analysis of the Ti-PILC support would indicate Na remaining, testing of that catalyst for NO reduction would show a corresponding lower NO conversion. The large increase in the BET surface area of the clay material upon pillaring (from 30 m²/g to 279 m²/g) further confirms the incorporation of TiO₂ into the clay structure. Using a high surface area support such as the TiO₂ pillared clay should ensure a better Pd dispersion.

4.2.2 Reaction Studies

Reaction studies were carried out according to the procedure described in section 2.2.1. Typically, a feed containing 3000 ppm H₂, 1000 ppm CO, 500 ppm NO, 5% O₂ with a total flow

rate of 200 mL/min is used, unless otherwise noted. The Pd dispersions were 27% for the 0.2 wt% Pd/Ti-PILC-B sample and 40% for the 0.1 wt% Pd/Ti-PILC-B sample, as determined by pulse O₂ chemisorption followed by pulse H₂ titration. The procedure for the titration experiment can be found in section 2.3.1.

4.3 Results and Discussion

4.3.1 Effect of Pd Loading on SCR of NO_x using a Simulated H₂-CO feed

The reduction of NO by H₂ and CO was conducted over Pd/Ti-PILC-B catalysts containing 0.1-0.5 wt% Pd. The amount of catalyst used for each catalytic testing was equivalent to 0.0005 g Pd in each case. Fig. 4.1 shows the steady state NO conversion as a function of reaction temperature. Deactivation was not observed over the duration of testing. The 0.1 wt% Pd catalyst was the most active, and the maximum NO_x conversion was observed at 170 °C. These results differ somewhat from those reported by Qi et al. that showed a maximum activity that occurred at a lower temperature [6]. The cause of the difference was not investigated in detail, but could be due to differences in Pd dispersion (ref. 6 did not provide dispersion information) since the surface areas of the Ti-PILC supports were different between the two studies. Minor differences in catalytic behavior for the clay samples are not unusual since the final characteristic of the intercalated clay is known to be modified by slight variations in the preparation procedure [8].

The NO conversion, H₂ and CO consumptions, N₂ selectivity, and NO_x reduction efficiency for the various Pd catalysts at 140 °C and 170 °C are reported in Table 4.2. The data show that as the Pd loading increases (Pd dispersion decreases), the NO_x reduction efficiencies

decrease while the corresponding rates of H₂ and CO oxidation increase. This could be because on larger Pd particles (lower Pd dispersion), the number of sites for adsorption of CO or H₂ as well as for dissociation of molecular oxygen would be more than that on a smaller Pd particle. This implies that H₂ and CO oxidation would be more favorable over larger metal particles since there are fewer dissociated oxygen atoms available to react with the adsorbed reductant on a small particle. The effect of Pd particle size on CO oxidation has been shown by Martinez-Arias et al. experimentally using supported Pd catalysts between 0.05 – 1.0 wt% Pd [9]. In agreement with our results, the authors found that the Pd catalysts with higher Pd loadings to be more active for CO oxidation.

As shown in Fig. 4.1, the effect of the Pd loading is evident only for reaction temperatures below about 200 °C. This observation is consistent with the results of Macleod et al. [1] and Qi et al. [10]. These authors found two conversion maxima in the reduction of NO with a H₂-CO mixture over supported Pd catalysts. Macleod et al. proposed two distinct reaction pathways occurring over the different temperature regions: reduction of NO by the in situ generation of NH₃ for the low temperature reaction pathway (below 200 °C) and the direct reduction of NO by H₂ at higher temperatures. More importantly, Qi et al. showed that Pd is not required for the second NO conversion peak by demonstrating that the 1%Pd-5%V₂O₅/TiO₂/Al₂O₃ catalyst and the 5%V₂O₅/TiO₂/Al₂O₃ catalyst both had comparable activity for NO reduction by hydrogen between 250 °C to 350 °C. Therefore our results suggest that, below 200 °C, lean NO reduction by H₂-CO is a structure sensitive reaction in which the Pd particle size plays a critical role.

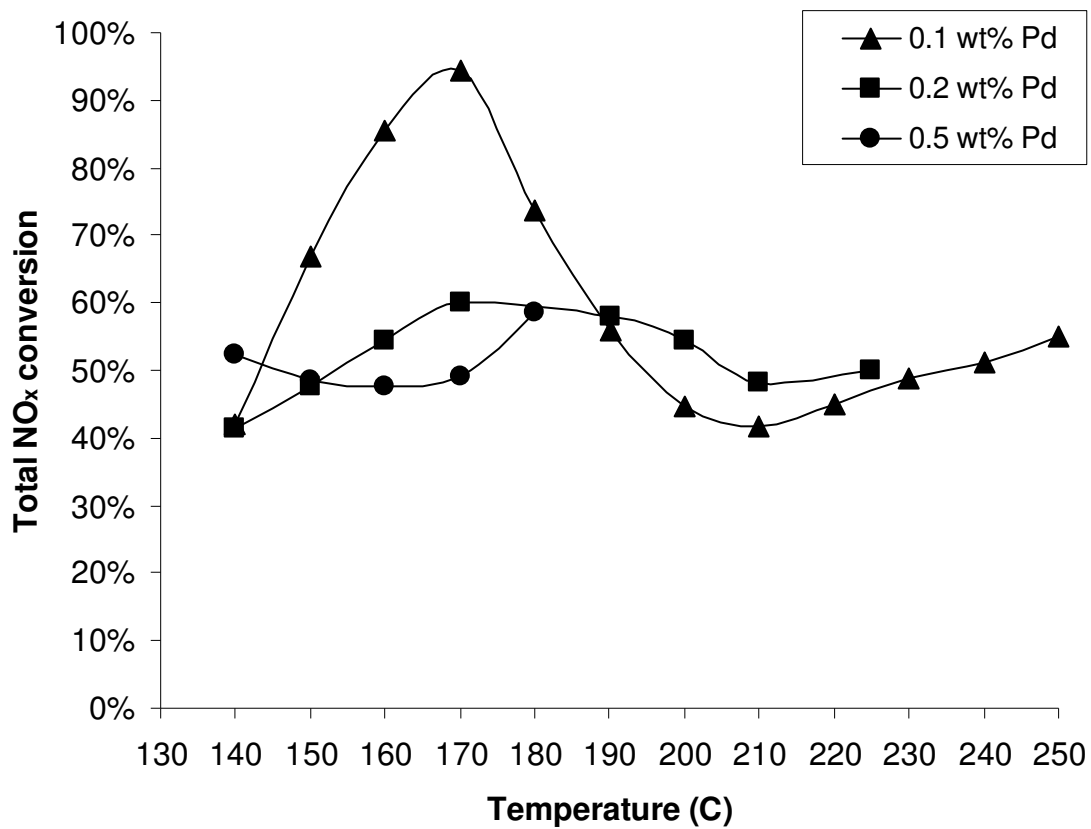


Figure 4.1 NO_x reduction with Pd/Ti-PILC-B catalysts as a function of temperature. Reaction conditions: 500 ppm NO, 3000 ppm H₂, 1200 ppm CO, 5% O₂, total flow rate 210 mL/min. In each case, the amount of catalyst used corresponds to 0.0005g Pd.

The role of Pd particle size is substantiated by examining the proposed reaction mechanism. NO dissociation on Pd has been proposed to be the initial step of the NO reduction reaction [4], and is likely the rate-determining step when the CO coverage is high [11]. Moreover, the dissociation of NO is a structure sensitive reaction, one that occurs more extensively on smaller Pd particles [12]. It has been postulated that NO dissociation proceeds with the assistance of an adsorbed hydrogen atom. Electron donation from adsorbed hydrogen to Pd would result in increased $d \rightarrow \pi^*$ back donation thereby weakening the N–O bond. This would lead to a significant increase in the rate of NO dissociation. Enhancement in the rate of NO dissociation in the presence of hydrogen has been reported previously by Hecker and Bell for supported Rh catalysts [13].

In relation to this, Macleod and coworkers found that at 100 °C, the temperature of maximum NO conversion, adsorption and subsequent dissociation of NO took place on reduced Pd (Pd^0) sites. Using in situ DRIFT, the authors identified NO adsorbed on reduced Pd ($\text{Pd}^0\text{-NO}$) at 1733 cm^{-1} [14]. Pd should be in its oxidized form initially. This assumption is reasonable considering that the final step in the catalyst preparation is calcination in an oxidizing atmosphere. In situ XANES studies have shown the evolution from a PdO state to a metallic Pd state during an experiment performed with a CO-O₂-NO mixture [15]. It can then be expected that under our reaction conditions, the Pd reduction process would take place during the course of the reaction as the Pd catalyst is exposed to the reaction mixture. This reduction process may depend to some extent on the degree of interaction between the oxidized Pd species and the Ti-PILC support. In principle, it should be easier to reduce the oxidized Pd species as they decrease in size [16]. Over our most active catalysts, it has been observed on numerous occasions that for

the first 10 to 15 minutes that the catalyst is exposed to the reaction mixture, there is a concurrent increase in the NO conversion monitored by the NO_x analyzer.

As was observed by Tauster et al. [17], it was also found that H₂ chemisorption was suppressed on highly dispersed Pd samples during our preliminary dispersion measurements (this led to the use of O₂-H₂ titration measurements instead). This anomalous reduction in hydrogen chemisorption capacity is a characteristic of the strong metal-support interaction (SMSI) effect [18]. One of the models used to explain this phenomenon proposes that strongly chemisorbed hydrogen remains on the metal surface after reduction and evacuation. Therefore, the surface Pd metal atoms are rendered inaccessible to further H₂ adsorption. Titania-supported metal catalysts are known to exhibit the SMSI effect. It is possible that as the reaction proceeds, NO adsorption is more competitive on the 0.1 wt% Pd samples due to the lower coverage of hydrogen.

Table 4.2. Effect of Pd loading on NO_x reduction, CO and H₂ conversions, N₂ selectivity, NO_x reduction efficiencies.

Catalyst	NO Conversion (%)		CO Conversion (%)		H ₂ Conversion (%)		N ₂ Selectivity (%)		NO _x Efficiencies	
	140 °C	170 °C	140 °C	170 °C	140 °C	170 °C	140 °C	170 °C	140 °C	170 °C
Temperature										
0.1Pd/Ti-PILC	44	94	5	91	23	100	76	88	0.30	0.15
0.2Pd/Ti-PILC	42	61	15	61	46	90	79	87	0.14	0.11
0.5Pd/Ti-PILC	52	44	44	100	85	100	84	90	0.10	0.08

Reaction conditions: 3000 ppm H₂, 1200 ppm CO, 500 ppm NO, 5% O₂, total flow rate 200 mL/min.

^aNO_x efficiencies = NO converted/H₂ consumed

4.3.2 Nitrogen Selectivity for H₂-CO SCR of NO

Unlike NO_x reduction efficiency, N₂ selectivity improved as the temperature increased from 140 °C to 170 °C. Assuming that N₂O formation is a reaction between a dissociated N atom and a NO molecule, then the rate of N₂O formation would be dependent on the concentration of adsorbed NO. NO coverage at any given time would be closely related to the rate of NO dissociation. Increase in the rate of NO dissociation would lead to a corresponding decrease in the concentration of adsorbed NO. Since the rate of N₂ formation increases with temperature (implying an increase in the rate of NO dissociation), the selectivity to N₂O would decrease as the reaction temperature increases.

Within error, the N₂ selectivity did not depend on the Pd particle size. This is in agreement with the literature report for H₂-SCR with supported Pt catalysts where the N₂ selectivity was found not to depend on the active metal properties, but on the acidity of the support, being higher on more acidic supports due to a higher concentration of adsorbed NH₄⁺ ions that could reduce NO as in NH₃-SCR [19, 20]. This would explain the higher selectivity observed with the Pd/Ti-PILC compared to Pd supported on individual oxides such as alumina or titania. Other than the influence of the support, addition of alkali elements such as potassium has been reported to promote the N₂ selectivity of Pd-based catalysts for NO_x reduction by CO + H₂ [21]. The alkali enhances the adsorption of NO and weakens the N–O bond in the adsorbed NO molecules, thus promoting the NO dissociation rate.

4.3.3 Effect of H₂O on NO_x Reduction Activity

The effect of water on the NO_x reduction activity at 185 °C is shown in Table 4.3. Addition of 4% H₂O caused the NO_x conversion to drop from 73% to 44%, most likely due to competitive adsorption by water. This loss in NO_x activity is fully reversible and can be recovered once water is removed from the feed as shown in Figure 4.2. The lower NO_x conversion in the presence of water is accompanied by a marked decrease in CO conversion, while the H₂ conversion remained high. Vannice and co-workers have shown that CO adsorption on Pd is weaker than H₂ adsorption to the extent that H₂ can displace CO on Pd/TiO₂ [22, 23]. This could account for the observation that water did not affect H₂ conversion as CO conversion. This would also imply that H₂ oxidation is more facile than CO oxidation. Referring to Table 4.2, the hydrogen consumption under most conditions is much higher than CO consumption, even in the absence of water.

Table 4.3

Effect of H₂O on the NO_x Reduction Activity at 185 °C.

Water Conc. (%)	NO Conversion (%)	CO Conversion (%)	H ₂ Conversion (%)	N ₂ Selectivity (%)
0	73	42	98	85
4	44	14	97	85

Reaction conditions: 3000 ppm H₂, 1400 ppm CO, 470 ppm NO, 5% O₂, total flow rate 200 mL/min, 0.5 g 0.1 wt% Pd/Ti-PILC-A.

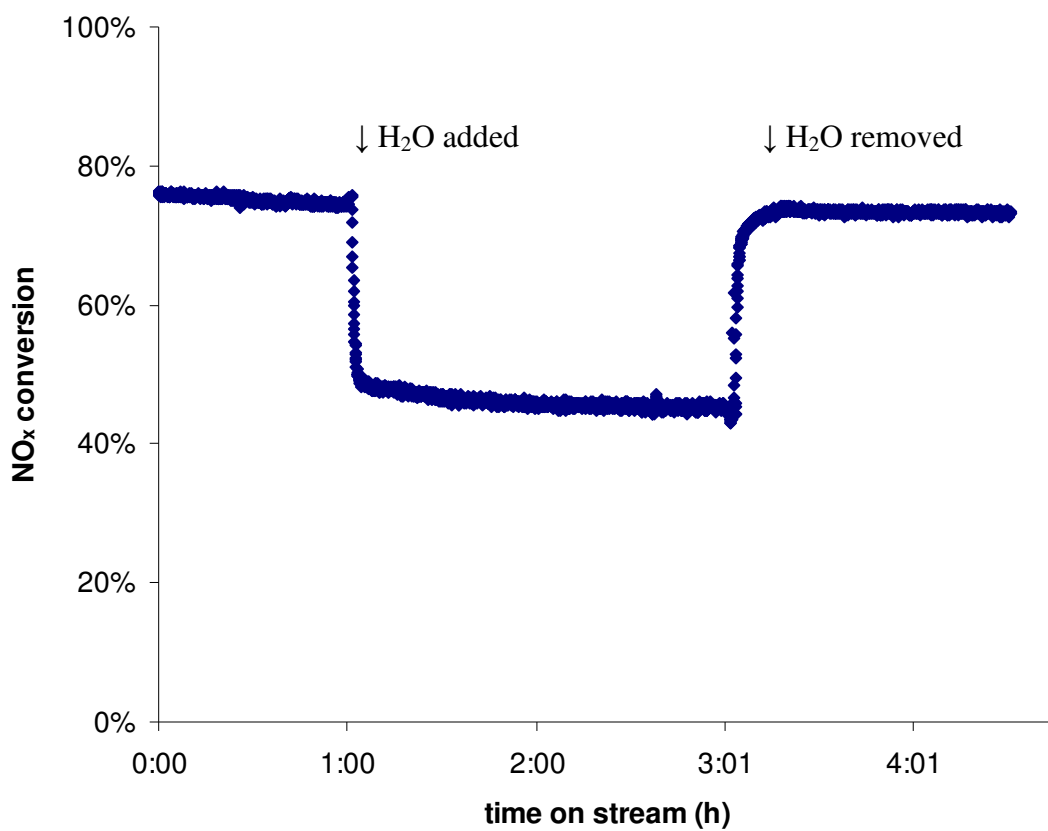


Figure 4.2. Effect of water on NO_x reduction at 185 °C. Reaction conditions: 3000 ppm H₂, 1400 ppm CO, 470 ppm NO, 5% O₂, 4% H₂O, total flow rate 200 ml/min, 0.5g 0.1wt% Pd/Ti-PILC-A.

4.4 Conclusions

It has been shown that the NO reduction activity increases as the Pd loading on the Pd/Ti-PILC catalysts decreases. Results from chemisorption studies confirm a higher Pd dispersion on the 0.1 Pd/Ti-PILC sample than the catalyst with a higher Pd loading such as the 0.2 Pd/Ti-PILC sample. Our finding indicates that Pd particle size is the key parameter controlling the NO_x activity. These results provide a reason for the large variation in the deNO_x catalytic activity over Pd catalysts on different supports as well as catalysts of similar composition but prepared using different Pd precursors. Water suppressed the deNO_x activity, but the effect was reversible and the activity could be recovered after removal of H₂O. The reduction in NO conversion is likely due to competitive adsorption between water molecules and CO.

CHAPTER 5: LOW TEMPERATURE LEAN NO_x REDUCTION BY COUPLING ETHYLENE GLYCOL REFORMING WITH SCR

5.1 Introduction

Based on recent developments in hydrocarbon reforming with high selectivity to hydrogen [1] and low temperature catalytic reduction of NO by H₂ [2], a novel strategy for NO_x abatement has been proposed. The novelty of this approach is the use of ethylene glycol reforming to produce H₂ for NO_x reduction. This coupled system is composed of two separate units: an ethylene glycol reforming unit to convert a mixture of ethylene glycol and water to H₂ followed by a separate H₂-deNO_x unit.

Previously, the feasibility of gas phase reforming of ethylene glycol (EG) as a separate unit preceding the deNO_x unit has been demonstrated [3]. The hydrogen generated from the reforming reaction would be sufficient for effective selective catalytic reduction (SCR) of NO. As supporting information, NO_x reduction was first studied using a simulated feed of H₂ and CO mixture using a Pd supported on titania pillared clay (Pd/Ti-PILC) catalyst. These results were presented in the previous chapter.

The objective of this work is to couple the EG reforming process to a lean NO_x reduction process to investigate the effect on NO_x removal using reductants (H₂/CO) derived from ethylene glycol reforming. In the integration of the reformer to the NO_x reduction system, it is important to recognize the requirements of the latter system. In this respect, two different deNO_x catalysts will be studied for this coupled EG-deNO_x system, a Pd supported on titania (Pd/TiO₂) catalyst

and a Pd/Ti-PILC catalyst. The effect of the reforming conditions on the NO_x performance was also examined.

5.2 Experimental

5.2.1 Catalyst

A Na-Pt/ γ -Al₂O₃ catalyst (1.4 wt% Na, 1 wt% Pt), identical to the one used previously, was used for EG reforming. It was prepared according to the procedure described in section 2.1. For the Pd/Ti-PILC catalysts, two batches of Ti-PILC support prepared with different amounts of Ti were made and used (refer to section 2.1.6 for a detail description of the preparation procedure).

5.2.2 Reaction Studies

Reaction studies were carried out according to the procedure described in section 2.2.1. For NO_x reduction using EG reformat in the coupled system, the reformat stream leaving the reforming reactor was combined with a simulated exhaust stream containing NO, O₂ and N₂, such that the 200 mL/min stream entering the NO_x reactor was composed of 3640–14000 ppm H₂, 0–3200 ppm CO, 2.9–6.8% H₂O, 500 ppm NO, and 5–5.8% O₂. All NO_x conversions reported here are steady state values obtained after at least 1 hr of reaction.

5.3 Results and Discussion

5.3.1 Coupled EG Reforming and deNO_x Reactions

All experiments with the coupled systems were carried out using 0.5g of the 0.1 wt% Pd/Ti-PILC catalyst for deNO_x, and the Na-Pt/ γ -Al₂O₃ catalyst for EG reforming. The gas composition was adjusted so that the feed to the deNO_x unit always contained ~500 ppm NO, ~5.5% O₂, with variable amounts of H₂, CO, and H₂O depending on the EG reforming condition.

Figure 5.1 shows the NO conversion for a 2.2% EG feed to the reformer. The ratio of oxygen to EG to the reformed was 1.2. As expected, there was significant NO_x conversion. However, the activity declined with time-on-stream, and 1/3 of the activity was lost in an hour. The NO conversion increased with higher EG concentration used (Table 5.1), which is expected because of higher concentrations of H₂ and CO produced. For the experiments listed in Table 5.1, deactivation of the deNO_x catalyst was also observed.

Since the Pd catalyst did not deactivate when a simulated reforming feed was used, we proposed that the observed deactivation is associated with the small amounts of unconverted EG, which was detected in these experiments. Although a small amount of methane is also present in the reformer effluent, it is unlikely to cause deactivation of the Pd catalyst. To determine if exposure to EG deactivates the catalyst and if the deactivation is reversible, a Pd catalyst was first tested with a simulated reforming feed containing H₂ and CO. Then it was used with an EG reformat identical as that shown in Figure 5.1, such that the deNO_x feed containing 0.1% EG would pass over the catalyst for 3 hr. Afterwards, the sample was purged with 150 mL/min gas mixture containing 6.7% O₂ balance N₂ for 5 hr at 170 °C to remove any material that might

have condensed in the pores. Following the purge, the deNO_x activity was tested again using the simulated reforming feed.

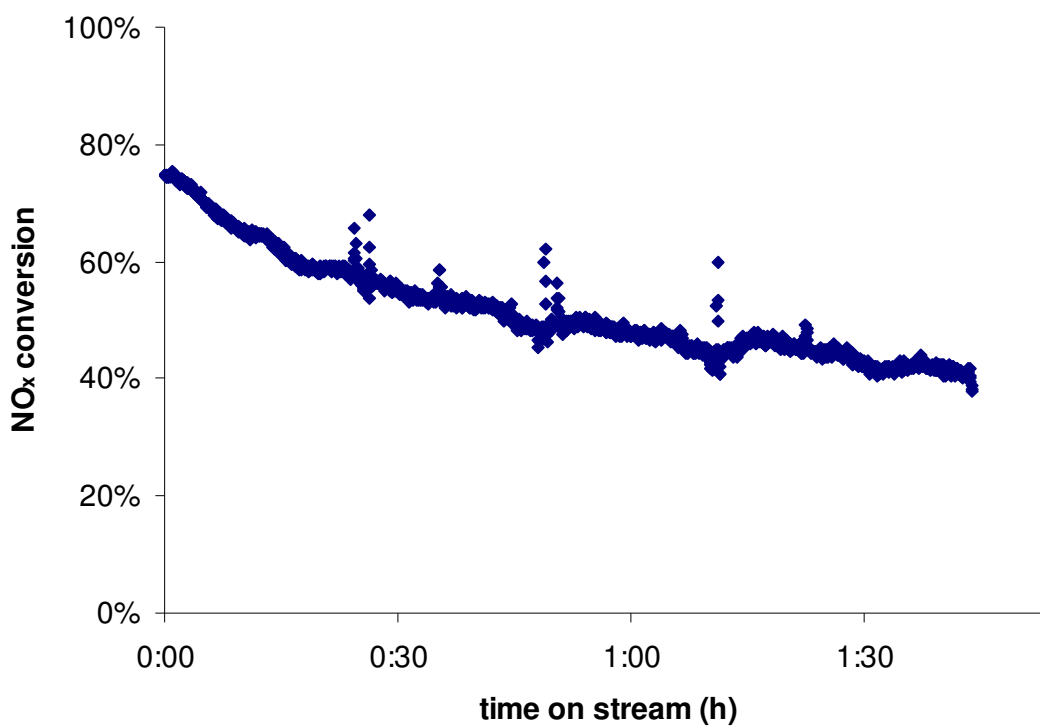


Figure 5.1

Coupled EG reforming-deNO_x reduction reaction. Reaction conditions for EG reforming: a feed of 2.2% EG, 2.65% O₂, 13.7% H₂O, total flow rate 77 mL/min, 0.1g Na-Pt/Al₂O₃ catalyst, 230 °C. Reaction conditions for coupled-deNO_x: a feed of 1.4 % H₂, 3200 ppm CO, 1100 ppm EG, 500 ppm NO, 5.3% O₂, 5.3% H₂O, total flow rate 200 mL/min, 0.5g 0.1wt% Pd/Ti-PILC-B, 170 °C.

The results (Table 5.2) show that exposure to unreacted EG deactivates the catalyst irreversibly under our conditions. The Pd catalyst had lost close to 80% of its original activity while the nitrogen selectivity remained unchanged. It is unlikely that with a longer purge time the catalyst will regain some of its NO reduction activity. The results imply that deactivation is not due to pore plugging of the catalyst. If access to 80% of the active sites has been blocked, leading to a subsequent decrease in NO conversion to the observed level, the CO conversion should be affected in the same manner. However, a comparison of the NO conversions and CO conversions for the catalyst before deactivation and the deactivated catalyst suggests that an intrinsic change to the Pd catalyst had taken place. Along with the decrease in the NO_x activity, the catalyst sample also changed color from yellow to gray, suggesting deposition of carbonaceous compounds as a possible cause of deactivation.

Table 5.1

Effect of EG Concentration in the Reformer on NO_x Conversion at 170 °C in the Coupled Reactor Unit.

EG reforming unit			deNO _x unit		
EG feed conc. ppm	O ₂ /EG	EG Conv. (%)	H ₂ Conc. ppm	CO Conc. ppm	NO Conv. (%)
3630	1.6	78	3640	390	48
4700	1.5	75	5600	520	70

Other reaction conditions for the deNO_x unit: 6.8% H₂O, 470 ppm NO, 5% O₂, total flow rate 200 mL/min, 0.3 g Na-Pt/Al₂O₃.

Table 5.2
Effect of Exposure to Ethylene Glycol on the NO_x Activity of Pd/Ti-PILC at 170 °C.

	NO Conversion (%)	CO Conversion (%)	H ₂ Conversion (%)	N ₂ Selectivity (%)
Before EG	94	91	100	88
After EG	21	49	83	86

Reaction conditions: 3000 ppm H₂, 1400 ppm CO, 490 ppm NO, 5% O₂, total flow rate 200 mL/min, 0.5 g 0.1 wt% Pd/Ti-PILC-B.

Experiments were then conducted to find conditions where ethylene glycol (EG) conversion is complete in the reforming unit by changing the EG and O₂ concentrations in the reforming feed. Table 5.3 shows the results of changing the EG concentration. Increasing the EG concentration from 3.5 to 8.2% did not affect the EG conversion significantly. On the other hand, increasing the O₂/EG ratio increased the EG conversion, eventually attaining 100% conversion for a ratio of 2.0 (Table 5.4). The initial conditions for reforming (O₂/EG ~ 1.2) in the coupled system were selected because it was previously found that operating under such conditions gives the highest H₂ production efficiency. As the O₂/EG ratio increases from 1.2 to 2.0, the H₂ production efficiency decreases from 2.6 to 1.5 most likely due to oxidation of the hydrogen.

Table 5.3

Effect of EG Concentration on the EG Conversion and H₂ Efficiency in EG Reforming.

EG Concentration (%)	EG Conversion (%)	H ₂ /EG	CO/CO ₂
3.5	71	1.85	0.30
5.0	68	1.84	0.31
8.2	68	1.68	0.55

Reaction Conditions: 0.1g Na-Pt/Al₂O₃, O₂/EG = 1.0, H₂O/EG = 6.2, total flow rate = 30 -49 mL/min, 230 °C.

Table 5.4

Effect of O₂/EG ratio on EG Reforming over 0.3g Na-Pt/Al₂O₃, total flow rate 45 mL/min, 230 °C.

EG Concentration (%)	O ₂ /EG	H ₂ O Concentration (%)	H ₂ formed (%)	CO formed (%)	EG Conversion (%)
0.89	1.2	16.5	2.3	0.105	86
0.73	1.5	13.7	1.8	0.026	93
0.57	2.0	10.7	0.87	0	100

Using the conditions derived from these experiments, the deNO_x reaction using the coupled reaction unit was tested again, and the results are shown in Figure 5.2. Unlike the previous tests, a stable activity was attained for the duration of the test. This indicates that deactivation is most likely due to ethylene glycol. Under the present reaction conditions, 450 ppm unreacted H₂ and 300 ppm unreacted CO were detected in the effluent from the deNO_x unit.

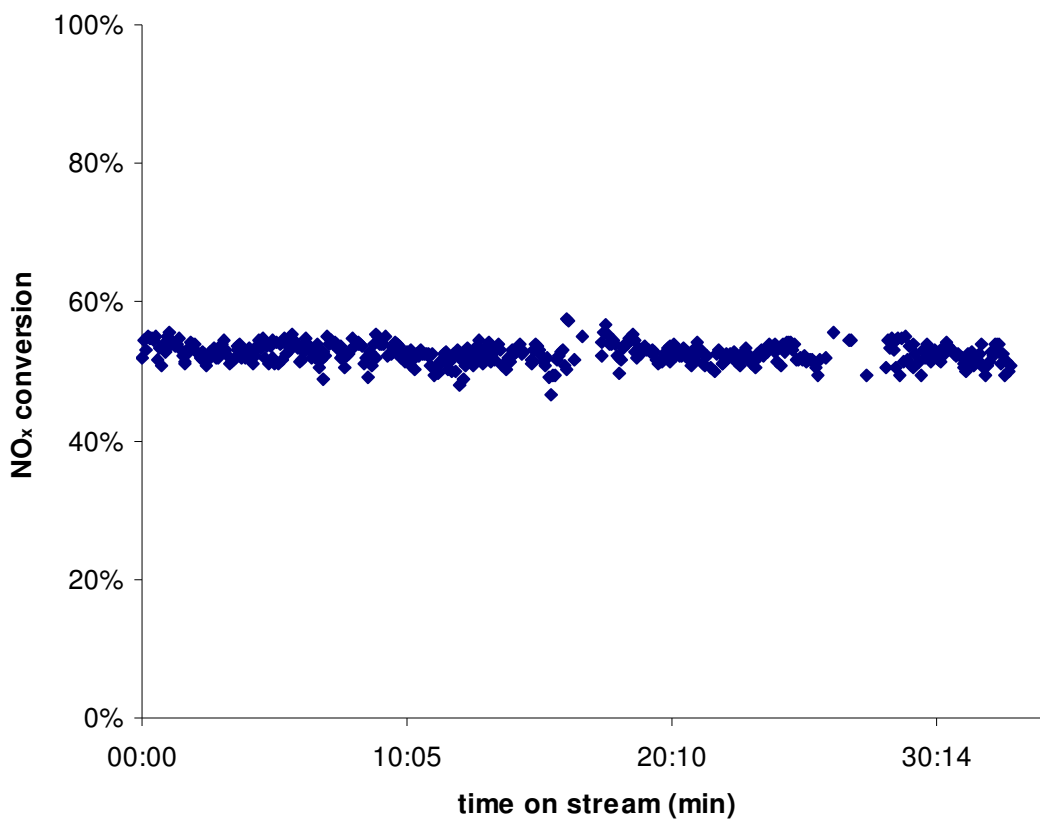


Figure 5.2

Coupled EG reforming-deNO_x reduction reaction. Reaction conditions for EG reforming: a feed of 1.36% EG, 2.8% O₂, 8.5% H₂O, total flow rate 71 mL/min, 1.0g Na-Pt/Al₂O₃ catalyst, 230 °C. Reaction conditions for coupled-deNO_x: a feed of 5400 ppm H₂, 960 ppm CO, 490 ppm NO, 5.8% O₂, 2.9% H₂O, total flow rate 200 mL/min, 0.5g 0.1wt% Pd/Ti-PILC-A, 185 °C.

The Pd/Ti-PILC catalyst achieves a much higher NO conversion when some CO is present [4]. However, when the O₂/EG ratio to the reforming unit is 2.0, no CO is detected in the product stream from the reformer. Under such conditions, the source of CO for NO reduction would come solely from the low concentrations of CO present in the diesel exhaust.

5.4 Conclusions

The reduction of NO_x at 185 °C on Pd supported on Ti-pillared clay was studied using H₂ and CO generated by reforming of ethylene glycol (EG) over a Na-Pt/γ-Al₂O₃ catalyst. It was found that for a stream containing 490 ppm NO, 5.8% O₂, and 2.9% H₂O, a stable NO_x conversion of ~55% was obtained when a stream of 1.36% EG was reformed under a condition that the EG conversion was complete and sufficient H₂ and CO was produced. However, if the EG conversion was incomplete, the unreacted EG deactivated the deNO_x catalyst, possibly by coking, that could not be regenerated by O₂ treatment at reaction temperature.

CHAPTER 6: CONCLUSIONS AND RECOMMENDATIONS FOR FUTURE WORK

6.1 Conclusions

In recent years, there has been a growing interest in using hydrogen as a NO_x reductant for SCR after the remarkable activity and selectivity of supported Pd catalysts have been discovered. Although outstanding work have been carried out, questions concerning the origin of the catalytic activity for NO reduction still remains to be answered. The main goal of this study is to understand this aspect of supported Pd catalyst and obtain insight into the active site for NO reduction. Another goal of this work is to investigate gas phase EG reforming for H_2 generation. More specifically, the aim for this portion of the work is to determine the effect of the reaction conditions, namely the oxygen and water concentrations on the H_2 production as well as the effect of Na modification to the $\text{Pt}/\text{Al}_2\text{O}_3$ reforming catalyst.

The Pd/Ti-PILC catalyst with the lowest Pd weight loading (0.1 wt% Pd) was the most active catalyst, achieving close to complete NO conversion with N_2 selectivity approaching 90%. Characterization of these catalysts by H_2 - O_2 titration showed that the 0.1 wt% sample had a higher Pd dispersion than the sample with a higher Pd loading, indicating that low temperature NO reduction by H_2 is a structure sensitive reaction. Before exposure of the 0.1 wt% Pd sample to the reaction mixture, it is reasonable to assume that the prepared Pd samples contained mostly PdO species. For the most active Pd catalysts, there is a period of activation, in which a gradual increase in the NO conversion is observed in the first 10 – 15 minutes of reaction. It is likely that this activation process involves the gradual transformation of the PdO species, possibly by H_2 , to reduced Pd (Pd^0) when it is exposed to the reaction mixture. The activation behavior was

not observed for the less active samples, indicating that the Pd reduction is less facile for larger Pd particles.

In addition, H₂ adsorption was greatly suppressed over the 0.1wt% sample, which could explain the higher NO_x efficiency over this sample. Taking all these together, small reduced Pd particles are likely the active centers for the H₂-CO SCR reaction.

For EG reforming, Na modification of the Pt/Al₂O₃ catalyst led to higher H₂ production and CO₂ formation. The promotion by Na was not due to change in Pt dispersion. Our model for the Na enhancement of EG reforming is as follows. Sodium, having a low ionization energy, will tend to transfer electrons to Pt. The more electron rich Pt will reduce the extent of bonding of electropositive compounds such as ethylene glycol and CO and strengthen its bonding with electronegative compounds such as oxygen. Since H₂ formation via dehydrogenation of ethylene glycol would require empty sites next to the sites in which ethylene glycol is adsorbed, a catalyst surface that is not saturated with ethylene glycol would result in more efficient H₂ production. Therefore, the function of Na is to modify the relative coverage of the reactants. Addition of oxygen prevents deactivation leading to a higher EG conversion but a lower H₂ production efficiency compared to reforming in the absence of oxygen. The lower H₂ production efficiency could be due to reaction of hydrogen with oxygen leading to an increase in the temperature of the catalyst bed. The effect of water on H₂ production is more complicated. A higher water content in the reforming feed led to higher H₂ production but the increase is not from the water-gas shift reaction. Rather, it could be that water affects the relative coverage of the reactants on the catalyst.

When the H_2 for NO reduction was derived from the reforming reaction, deactivation of the $deNO_x$ catalyst was observed. Deactivation was found to be caused by unreacted ethylene glycol from the reforming unit, since deactivation did not occur with a simulated H_2 -CO feed. The deactivation described here was found to be irreversible. The color change of the Pd catalyst from light yellow to gray indicates that deactivation is due to coking.

In summary, Pd particle size has been proposed as the parameter governing NO activity over supported Pd catalysts. Such a model is based on results from reaction studies using samples with different Pd loadings together with chemisorption measurements to determine the Pd dispersion over these catalysts. The variation in activities reported in the literature can be explained by this model. For the EG reforming reaction, addition of oxygen stopped deactivation. Na promotion over the reforming catalyst was observed. For the coupled system, it was found that the $deNO_x$ catalyst deactivates irreversibly upon exposure to EG. This problem could be resolved by increasing the O_2/EG ratio to 2.0 so that complete EG conversion is obtained.

6.2 Recommended Work.

6.2.1 H₂-CO SCR of NO

One of the most pressing matters for NO reduction is the effect of water on the NO reduction activity. Although there are reports on the catalyst performance in the presence of water, there have been no attempts to determine the intrinsic property of the pillared clay catalyst that determines its resistance to water. The Pd/Ti-PILC used for our study experienced a noticeable drop in NO conversion when water was present. This issue of suppression of NO_x reduction activity by water has been discussed in a review by Kim and Nam [1]. Modification of the zeolite support was cited as one approach to improve the resistance of the NO_x catalyst towards water.

It has been shown that the titania pillared clay support is highly dependent on the preparation procedure [2]. Although the process of pillaring by titania is highly complex, it is known that one key parameter to affect the final clay support is the concentration of Ti precursor added to the starting clay material. Given the high concentration of TiO₂ added to the clay (in our case the Ti-PILC contains around 40wt% TiO₂), it is reasonable to assume that besides the formation of TiO₂ pillars between the clay layers, TiO₂ is also distributed on the surface of the clay. Varying the amount of TiO₂ added to the clay would have a large effect on the pillaring, and thereby the support structure. This is one possible approach to determine if the resistance of pillared clay catalyst towards water can be modified by the support. Practically, it would be a useful piece of information since the water is one of the main components in the diesel exhaust as well as a product of reforming.

6.2.2 Ethylene Glycol Reforming

Addition of oxygen to the reforming feed was found to prevent deactivation of the catalyst when reforming was carried out at an EG concentration of 2.2%. This takes place at the expense of the H₂ production efficiency since this value is 3 in the absence of oxygen and only 1.6 for oxidative EG reforming. One way to increase the H₂ production efficiency is to increase the water gas shift (WGS) activity of the reforming catalyst. The ability of Na/Pt/Al₂O₃ to catalyze the WGS reaction is rather poor. Pt supported on CeO₂ is one of the most active catalyst for WGS but not an effective catalyst for aqueous phase reforming of EG. Formation of a ceria-alumina mixed support could provide a means to enhance the WGS activity without losing the reforming activity. Identification of the optimum surface ceria to alumina using different ceria to alumina ratios and/or preparation procedures could create a catalyst over which WGS and reforming proceeds efficiently.

REFERENCES

Chapter 1

1. J.N. Armor, *Appl. Catal. B* 1 (1992) 221.
2. J.N. Armor, *Catal. Today* 26 (1995) 99.
3. <http://epa.gov/air/urbanair/nox/what/html>
4. H. Wise, M.F. Frech, *J. Chem. Phys.* 20 (1952) 22.
5. M. Iwamoto, H. Furukawa, Y. Mine, F. Uemura, S.-i. Mikuriya, S. Kagawa, *J. Chem. Soc. Chem. Commun.* (1986) 1272.
6. F. Garin, *Catal. Today* 89 (2004) 255.
7. W. Held, A. Konig, T. Richter, L. Puppe, *SAE* (1990) No. 900496.
8. K.C. Taylor, *Catal. Rev.-Sci. Eng.* 35(4) (1993) 457.
9. C.H. Bartholomew, R.J. Farrauto, *Fundamentals of Industrial Catalytic Processes*, (2006) 719.
10. A. Kato, H. Yamashita, H. Kawagoshi, S. Matsuda, *Commun. Am. Ceram. Soc.* 70(7) (1987) C159.
11. M. Machida, K. Eguchi, H. Arai, *Bull. Chem. Soc. Japan* 61(10) (1988) 3659.
12. J. Dettling, H. Hwang, S. Pudick, S. Tauster, *SAE* 900506 (1990).
13. S. Matsumoto, *Cattech* 4 (2000) 102.
14. M. Shelef, G.W. Graham, *Catal. Rev.-Sci. Eng.* 36(3) (1994) 433.
15. K.C. Taylor, *Catalysis-Science and Technology* (J.R. Anderson and M. Boudart, Eds., Vol. 5), Springer-Verlag, Berlin, (1984) 119.

16. J. Leyrer, E.S. Lox, W. Strehlau, SAE 952495 (1995).
17. H.H. Kung, M.C. Kung, *Catal. Today* 30 (1996) 5.
18. A. Obuchi, A. Ohi, M. Nakamura, A. Ogata, K. Mizuno, H. Obuchi, *Appl. Catal. B* 2 (1993) 71.
19. K.C.C. Kharas, *Appl. Catal. B* 2 (1993) 207.
20. R.M. Heck, R.J. Farrauto, *Spec. Publ. R. Soc. Chem.* 139 (1994) 120.
21. www.dieselnet.com/standards/us/ld.php
22. www.dieselnet.com/standards/us/ld_t2.php
23. M. Iwamoto, H. Yahiro, Y. Yu-u, S. Shundo, N. Mizuno, *Shokubai* 32 (1990) 430.
24. W. Held, A. Konig, T. Richter, L. Puppe, *SAE Trans.* 4 No. 900496 (1990) 209.
25. Klingstedt, F.; Arve, K.; Eranen, K.; Murzin, D.Y.; *Accounts of Chemical Research* 39 (2006) 273.
26. N. Takahashi, H. Shinjoh, T. Iijima, T. Suzuki, K. Yamazaki, K. Yokota, H. Suzuli, N. Miyoshi, S. Matsumoto, T. Tanizawa, T. Tanaka, S. Tateishi, K. Kasahara, *Catal. Today* 27 (1996) 63.
27. W. Bogner, M. Kramer, B. Krutsch, S. Pischinger, D. Voigtlander, G. Wenninger, F. Wirbeleit, M.S. Brogan, R.J. Brisley, D.E. Webster, *Appl Catal. B* 7 (1995) 153.
28. L.J. Gill, P.G. Blakeman, M.V. Twigg, A.P. Walker, *Top. Catal.* 28 (2004) 157.
29. Epling, W.S.; Campbell, L.E.; Yezerets, A.; Currier, N.W.; Parks, J.E., *Catal. Rev.* 46 (2004) 163.
30. S. Poulston, R.R. Rajaram, *Catal. Today* 81 (2003) 603.

31. S.D. Yim, S.J. Kim, J.H. Baik, I.-S. Nam, Y.S. Mok, J.-H. Lee, B.K. Cho, S.H. Oh, *Ind. Eng. Chem. Res.* 43 (2004) 4856.
32. A. Kato, S. Matsuda, T. Kamo, F. Nakajima, H. Kuroda, T. Narita, *J. Phys. Chem.* 85 (1981) 4099.
33. I.-S. Nam, S.D. Yim, J.H. Baik, S.H. Oh, B.K. Cho, *US Patent Application* 10/723,306 (2003).
34. C. Ciardelli, I. Nova, E. Tronconi, D. Chatterjee, B. Bandl-Konrad, M. Weibel, B. Krutzsch, *Appl. Catal. B* 70 (2007) 80.
35. R.T. Yang, J.E. Cichanowicz, *U.S. Patent* 5,415,850 (1995).
36. L.S. Cheng, R.T. Yang, N. Chen, *J. Catal.* 164 (1996) 70.
37. R.T. Yang, W.B. Lin, *J. Catal.* 155 (1995) 414.
38. W.B. Li, M. Sirilumpen, R.T. Yang, *Appl. Catal.* 11 (1997) 347.
39. S. Perathoner, A. Vaccari, *Clay Minerals* 32 (1997) 123.
40. M. Iwamoto, H. Takeda, *Catal. Today* 27 (1996) 71.
41. R. Burch, P.J. Millington, A.P. Walker, *Appl. Catal. B* 4 (1994) 64.
42. K. Yokota, M. Fukui, T. Tanaka, *Appl. Surf. Sci.* 121/122 (1997) 273.
43. B. Frank, G. Emig, A. Renken, *Appl. Catal. B* 19 (1998) 45.
44. R. Burch, M.D. Coleman, *Appl. Catal. B* 23 (1999) 115.
45. A. Ueda, N. Takayuki, A. Masashi, T. Kobayashi, *Catal. Today* 45 (1998) 135.
46. A. Ueda, T. Nakao, M. Azuma, T. Kobayashi, *Chem. Lett.* (1998) 595.
47. K.C. Taylor, R.L. Klimisch, *J. Catal.* 30 (1973) 478.
48. W.C. Hecker, A.T. Bell, *J. Catal.* 92 (1985) 247.

49. E. Shustorovich, A.T. Bell, *Surf. Sci.* 289 (1993) 127.
50. R. Burch, T.C. Watling, *Catal. Lett.* 37 (1996) 51.
51. N. Macleod, R. Cropley, J.M. Keel, R.M. Lambert, *J. Catal.* 221 (2004) 20.

Chapter 2

1. K. Maeda, F. Mizukami, S. Niwa, M. Toba, *J. Chem. Soc. Faraday Trans.* 88 (1992) 97.
2. Y. Amenomiya, A. Emesh, K. Oliver, G. Pleizer, in: M. Philips, M. Ternan (Eds.), *Proceedings of the Ninth International Congress Catal.*, Chemical Institute of Canada, Ottawa, Canada, (1988) 634.
3. Y. Li, Q. Fu, M. Flytzani-Stephanopoulos, *Appl. Catal. B* 27 (2000) 179.
4. J. Sterte, *Clays Clay Miner.* 34 (1986) 658.
5. W.A. Dietz, *J. Gas Chromatogr.* (1976) 68.
6. M. Boudart, H.S. Hwang, *J. Catal.* 39 (1975) 44.
7. R.K. Usmen, R.W. McCabe, M. Shelef, *Stud. Surf. Sci. Catal.* 96 (1995) 789.

Chapter 3

1. N. Macleod, R. Cropley, R.M. Lambert, *Catal. Lett.* 86 (2003) 69.
2. S. Satokawa, *Chem. Lett.* (2000) 294.
3. N. Macleod, R. Cropley, J.M. Keel, R.M. Lambert, *J. Catal.* 221 (2004) 20.
4. D.J. Miller, J.E. Jackson, J.G. Frye, T.A. Werpy, S.P. Chopade, A.H. Zacher, U.S. Patent 6,291,725 2001.

5. J.W. Shabaker, G.W. Huber, R.R. Davda, R.D. Cortright, J.A. Dumesic, *Catal. Lett.* 88 (2003) 1.
6. W. Kim, T. Voithl, G.J. Rodriguez-Rivera, J.A. Dumesic, *Science* 305 (2004) 1280.
7. R.D. Cortright, R.R. Davda, J.A. Dumesic, *Nature* 418 (2002) 964.
8. N. Macleod, R.M. Lambert, *Catal. Commun.* 3 (2002) 61.
9. J.W. Shabaker, G.W. Huber, J.A. Dumesic, *J. Catal.* 222 (2004) 180.
10. R.R. Davda, J.W. Shabaker, G.W. Huber, R.D. Cortright, J.A. Dumesic, *Appl. Catal. B* 43 (2002) 13.
11. J.W. Shabaker, R.R. Davda, G.W. Huber, R.D. Cortright, J.A. Dumesic, *J. Catal.* 215 (2003) 344.
12. Q. Fu, H. Saltsburg, M. Flytzani-Stephanopoulos, *Science* 301 (2003) 935.
13. ICI, *Catalyst Handbook*, Wolfe London (1970) 64.
14. I.R. Harkness, R.M. Lambert, *J. Chem. Soc., Faraday Trans.* 93 (1997) 1425.
15. J.W. Niemantsverdriet, *Appl. Phys. A* 61 (1995) 503.
16. Y. Li, Q. Fu, M. Flytzani-Stephanopoulos, *Appl. Catal. B* 27 (2000) 179.
17. Y.-F. Yu Yao, *J. Catal.* 87 (1984) 152.
18. H. Iida, A. Igarashi, *Appl. Catal. A* 298 (2006) 152.
19. M. Konsolakis, N. Macleod, J. Isaac, I.V. Yentekakis, R.M. Lambert, *J. Catal.* 193 (2000) 330.
20. M. Kiskinova, G. Pirug, H.P. Bonzel, *Surf. Sci.* 133 (1983) 321.
21. K. Yokota, M. Fukui, T. Tanaka, *Appl. Surf. Sci.* 121/122 (1997) 273.
22. N. Macleod, J. Isaac, R.M. Lambert, *Appl. Catal. B* 33 (2001) 335.

23. C.-H. Lee, Y.-W. Chen, *Ind. Eng. Chem. Res.* 36 (1997) 1498.
24. A. Palermo, R.M. Lambert, I.R. Harkness, I.V. Yentekakis, O. Marina, C.G. Vayenas, *J. Catal.* 161 (1996) 471.
25. R.M. Lambert, F.J. Williams, A. Palermo, M.S. Tikhov, *Top. Catal.* 13 (2000) 91.

Chapter 4

1. N. Macleod, R.M. Lambert, *Catal. Commun.* 3 (2002) 61.
2. Y.-W. Lee, E. Gulari, *Catal. Commun.* 5 (2004) 499.
3. A. Ueda, T. Nakao, M. Azuma, T. Kobayashi, *Chem. Lett.* (1998) 595.
4. N. Macleod, R. Cropley, J.M. Keel, R.M. Lambert, *J. Catal.* 221 (2004) 20.
5. F. Solymosi, T. Bansagi, *J. Catal.* 202 (2001) 205.
6. G. Qi, R.T. Yang, L.T. Thompson, *Appl. Catal. A* 259 (2004) 261.
7. S. Matsumoto, *Cattech* 4 (2000) 102.
8. A. Bernier, L.F. Admaiai, P. Grange, *Appl. Catal.* 77 (1991) 269.
9. A. Martinez-Arias, A.B. Hungria, M. Fernandez-Garcia, A. Iglesias-Juez, J.A. Anderson, J.C. Conesa, *J. Catal.* 221 (2004) 85.
10. G. Qi, R.T. Yang, F.C. Rinaldi, *J. Catal.* 237 (2006) 381.
11. J.H. Miners, A.M. Bradshaw, P. Gardner, *Phys. Chem. Chem. Phys.* 1 (1999) 4909.
12. X. Xu, D.W. Goodman, *Catal. Lett.* 24 (1994) 31.
13. W.C. Hecker, A.T. Bell, *J. Catal.* 92 (1985) 247.
14. N. Macleod, R. Cropley, R.M. Lambert, *Catal. Lett.* 86 (2003) 69.

15. M. Fernandez-Garcia, A. Martinez-Arias, A. Iglesias-Juez, A.B. Hungria, J.A. Anderson, J.C. Conesa, J. Soria, *J. Catal.* 214 (2003) 220.
16. K. Otto, L.P. Haack, J.E. deVries, *Appl. Catal. B* 1 (1992) 1.
17. S.J. Tauster, S.C. Fung, R.L. Garten, *J. Am. Chem. Soc.* 100 (1978) 170.
18. G.B. Raupp, S.A. Stevenson, J.A. Dumesic, S.J. Tauster, R.T.K. Baker, *Metal-Support Interactions in Catalysis, Sintering and Redispersion* (1987) 76.
19. J. Shibata, M. Hashimoto, K. Shimizu, H. Yoshida, T. Hattori, A. Satsuma, *J. Phys. Chem. B* 108 (2004) 18327.
20. A. Satsuma, M. Hashimoto, J. Shibata, H. Yoshida, T. Hattori, *Chem. Commun.* (2003) 1698.
21. M. Konsolakis, M. Vrontaki, G. Avgouropoulos, T. Ioannides, I.V. Yentekakis, *Appl. Catal. B* 68 (2006) 59.
22. M.A. Vannice, S.Y. Wang, S.H. Moon, *J. Catal.* 71 (1981) 152.
23. S.Y. Wang, S.H. Moon, M.A. Vannice, *J. Catal.* 71 (1981) 167.

Chapter 5

1. J.W. Shabaker, G.W. Huber, R.R. Davda, R.D. Cortright, J.A. Dumesic, *Catal. Lett.* 88 (2003) 1.
2. N. Macleod, R.M. Lambert, *Catal. Commun.* 3 (2002) 61.
3. H.Y. Law, M.C. Kung, H.H. Kung, *Ind. Eng. Chem. Res.* 46 (2007) 5936.
4. G. Qi, R.T. Yang, L.T. Thompson, *Appl. Catal. A* 259 (2004) 261.

Chapter 6

1. M.-H. Kim, I.-S. Nam. *Catalysis* 18 (2004) 116.
2. A. Bernier, L.F. Admaiai, P. Grange, *Appl. Catal.* 77 (1991) 269.